

RESEARCH

Open Access



# Microglial morphological/inflammatory phenotypes and endocannabinoid signaling in a preclinical model of periodontitis and depression

Javier Robledo-Montaña<sup>1,2</sup>, César Díaz-García<sup>1,2</sup>, María Martínez<sup>3,4</sup>, Nagore Ambrosio<sup>3,4</sup>, Eduardo Montero<sup>3,4</sup>, María José Marín<sup>3</sup>, Leire Virto<sup>3,5</sup>, Marina Muñoz-López<sup>1,2</sup>, David Herrera<sup>3,4</sup>, Mariano Sanz<sup>3,4</sup>, Juan Carlos Leza<sup>1,2</sup>, Borja García-Bueno<sup>1,2</sup>, Elena Figuero<sup>3,4\*</sup> and David Martín-Hernández<sup>1,2\*†</sup>

## Abstract

**Background** Depression is a chronic psychiatric disease of multifactorial etiology, and its pathophysiology is not fully understood. Stress and other chronic inflammatory pathologies are shared risk factors for psychiatric diseases, and comorbidities are features of major depression. Epidemiological evidence suggests that periodontitis, as a source of low-grade chronic systemic inflammation, may be associated with depression, but the underlying mechanisms are not well understood.

**Methods** Periodontitis (P) was induced in Wistar: Han rats through oral gavage with the pathogenic bacteria *Porphyromonas gingivalis* and *Fusobacterium nucleatum* for 12 weeks, followed by 3 weeks of chronic mild stress (CMS) to induce depressive-like behavior. The following four groups were established ( $n = 12$  rats/group): periodontitis and CMS (P + CMS+), periodontitis without CMS, CMS without periodontitis, and control. The morphology and inflammatory phenotype of microglia in the frontal cortex (FC) were studied using immunofluorescence and bioinformatics tools. The endocannabinoid (EC) signaling and proteins related to synaptic plasticity were analyzed in FC samples using biochemical and immunohistochemical techniques.

**Results** Ultrastructural and fractal analyses of FC revealed a significant increase in the complexity and heterogeneity of Iba1 + parenchymal microglia in the combined experimental model (P + CMS+) and increased expression of the proinflammatory marker inducible nitric oxide synthase (iNOS), while there were no changes in the expression of cannabinoid receptor 2 (CB2). In the FC protein extracts of the P + CMS+ animals, there was a decrease in the levels

†Elena Figuero and David Martín-Hernández as joint senior authors.

\*Correspondence:

Elena Figuero  
elfiguer@ucm.es  
David Martín-Hernández  
davidmhbiotec@gmail.com

Full list of author information is available at the end of the article

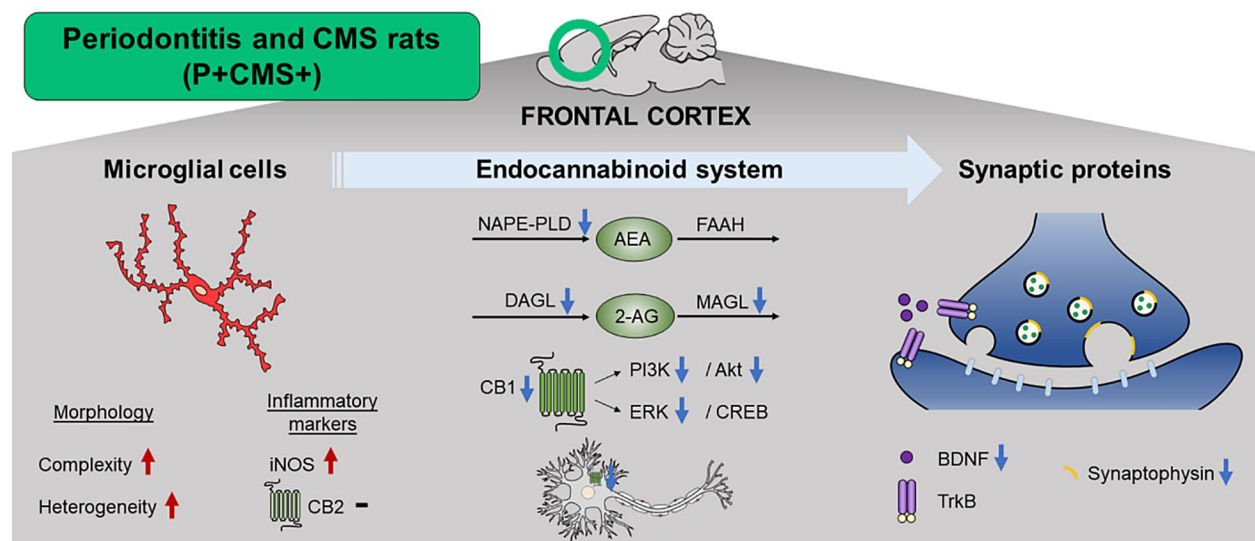


© The Author(s) 2024. **Open Access** This article is licensed under a Creative Commons Attribution-NonCommercial-NoDerivatives 4.0 International License, which permits any non-commercial use, sharing, distribution and reproduction in any medium or format, as long as you give appropriate credit to the original author(s) and the source, provide a link to the Creative Commons licence, and indicate if you modified the licensed material. You do not have permission under this licence to share adapted material derived from this article or parts of it. The images or other third party material in this article are included in the article's Creative Commons licence, unless indicated otherwise in a credit line to the material. If material is not included in the article's Creative Commons licence and your intended use is not permitted by statutory regulation or exceeds the permitted use, you will need to obtain permission directly from the copyright holder. To view a copy of this licence, visit <http://creativecommons.org/licenses/by-nc-nd/4.0/>.

of the EC metabolic enzymes N-acyl phosphatidylethanolamine-specific phospholipase D (NAPE-PLD), diacylglycerol lipase (DAGL), and monoacylglycerol lipase (MAGL) compared to those in the controls, which extended to protein expression in neurons and in FC extracts of cannabinoid receptor 1 (CB1) and to the intracellular signaling molecules phosphatidylinositol-3-kinase (PI3K), protein kinase B (Akt) and extracellular signal-regulated kinase 1/2 (ERK1/2). The protein levels of brain-derived neurotrophic factor (BDNF) and synaptophysin were also lower in P+CMS+ animals than in controls.

**Conclusions** The combined effects on microglial morphology and inflammatory phenotype, the EC signaling, and proteins related to synaptic plasticity in P+CMS+ animals may represent relevant mechanisms explaining the association between periodontitis and depression. These findings highlight potential therapeutic targets that warrant further investigation.

### Graphical Abstract



**Keywords** Depression, Periodontitis, Microglia, Endocannabinoid signaling, Synaptic plasticity

### Background

Major depressive disorder (MDD) is a serious neuropsychiatric disease characterized by a depressed mood, impaired cognition, and vegetative dysfunctions [1]. Depressive disorders affect approximately 3.8% of the global population and are more prevalent in women [2]. The World Health Organization (WHO) has projected that depression will emerge as the leading cause of disability-adjusted life years (DALYs) by 2030 [3], but the aftermath of the COVID-19 pandemic may even exacerbate the importance of mental health within overall public health [4]. Indeed, the sociosanitary burden is sizable (\$333.7 billion in the US in 2019 [5]), particularly for treatment-resistant patients [6], who are associated with 58.5% higher total costs [7].

Despite the evidence suggesting the involvement of biological and environmental factors in its etiology, a complete understanding of MDD pathophysiology remains elusive [8]. Notably, exposure to physical and psychological stressors that activate inflammatory mechanisms

when persistent and uncontrolled may affect mood-controlling pathways in the brain at multiple levels, hampering physiological functions and affecting both function and structure [9].

In recent years, epidemiological evidence has substantiated the significant comorbidity between psychiatric disorders and chronic systemic inflammatory diseases [10]. Notably, periodontitis, arising from a dysbiotic subgingival microbiome challenging the host response, and being a source of low-grade inflammation, may be recognized as an independent potential contributor to mental health [11]. However, the nature of this association, whether causal or otherwise, and the specific mechanisms involved remain unclear. Over the last few years, our research, along with that of others, has aimed to unravel the role of the oral-brain axis in psychiatric diseases [11].

Specifically, our investigations revealed the presence of the periodontal pathogenic bacteria *Fusobacterium nucleatum*, neuroinflammation, alterations in

the expression of key mediators regulating blood–brain barrier (BBB) permeability, and the modulation of sphingosine-1-phosphate (S1P) signaling in the frontal cortex (FC) of rats exposed to a combined model of periodontitis (oral gavage with periodontal pathogens) and depression (chronic mild stress [CMS]) [12, 13]. In this experimental model, a notable hallmark of neuroinflammation was the increased microglial population in the FC, accompanied by qualitative changes in microglial microscopic morphology, suggesting an activated phenotype that warrants further investigation [12].

Microglia are resident cells within the central nervous system (CNS) parenchyma responsible for immune surveillance and are intimately related to the BBB through perivascular macrophages [14]. Clinical data from MDD patients and animal models have revealed that microglial activation is associated with symptoms [15, 16]. Furthermore, microglia respond to periodontitis by adopting an activated and proinflammatory phenotype [17]. However, it is crucial to recognize the diversity of microglial populations and functions beyond mere activation states [18]. The hypothesis that a specific type or profile of microglia is associated with specific disease stages and individual heterogeneity has ignited a debate fostering the search for precision medicine pathways [19]. While classical studies have focused on M1 proinflammatory and M2 anti-inflammatory microglial phenotypes, this binary approach may oversimplify their role. Some authors have reported controversial results in various neuropathological conditions, including psychiatric disorders [20–23], underscoring the need for a comprehensive multilevel classification to elucidate the distinct characteristics and roles of different microglial subpopulations [24].

Beyond immune surveillance, a significant role attributed to microglia is the regulation of crucial neurophysiological processes, such as synaptic plasticity. Dysregulation of synaptic plasticity could be a pertinent factor in the pathophysiology of MDD [25, 26]. One of the extensively studied modulators of microglial actions on neuronal synaptic plasticity is the homeostatic endocannabinoid (EC) system [27], which is also altered both in MDD and periodontitis.

The association between the EC system and MDD has been extensively studied [28]. Numerous reports have documented alterations in the levels of ECs in brain and peripheral samples of MDD patients [29] and in stress-based animal models [30]. Various psychiatric drugs upregulate the EC system [31], and the EC activity appears to be critical for the mechanism of newly developed rapid-action antidepressant therapies [32, 33]. EC signaling also plays a beneficial role directly in periodontal tissue [34]. Gingival biopsies from periodontitis patients have shown a decrease in cannabinoid receptor (CB) 2 [35], while cannabinoid-based interventions

have been found to reduce gum inflammation [36, 37], enhance periodontal regeneration [38], and promote osteogenic differentiation [39]. Interestingly, inflammation caused by the lipopolysaccharide (LPS) of *Porphyromonas gingivalis* in human periodontal ligament cells is attenuated after EC methanandamide treatment [40], and the EC effects on these cells are similar to those observed in microglia [41]. This evidence suggests that the anti-inflammatory properties of ECs might constitute an indirect link between periodontitis and depression.

In essence, the EC system encompasses the ECs (arachidonate-based lipids), anandamide (AEA) [42] and 2-arachidonoylglycerol (2-AG) [43]; their cannabinoid receptor CB1 [44] and CB2 [45]; their two main synthesis enzymes, N-acyl phosphatidylethanolamine phospholipase (NAPE) and diacylglycerol lipase (DAGL); and their degradation or reuptake enzymes, fatty acid amide hydrolase (FAAH) and monoacylglycerol lipase (MAGL) [46].

CB1 is the predominant G-protein coupled receptor (GPCR) in the mammalian brain, while CB2 is highly expressed in immune cells [47]. Their activities are primarily associated with neuroprotective and anti-inflammatory actions, emphasizing the critical role of maintaining homeostatic EC balance for overall health and disease [48]. Notably, microglial CB2 is essential for establishing long-term memory and promoting an anti-inflammatory profile [49]. Downstream signaling by CB1 and CB2 involves several second messengers, including mitogen-activated protein kinases (MAPKs), such as phosphatidylinositol-3-kinase (PI3K), protein kinase B (Akt), and extracellular signal-regulated kinase (ERK). These pathways can activate cAMP response element-binding protein (CREB), which is implicated in cellular surveillance and plasticity [50].

Alterations in synaptic plasticity driven by microglia have been postulated to be a pathophysiological mechanism underlying depression [51]. Two pivotal molecules in these processes are brain-derived neurotrophic factor (BDNF) and synaptophysin. Along with its polymorphism (Val66Met), BDNF plays a role in mediating antidepressant effects in both patients and preclinical models [52, 53], while low levels of synaptophysin correlate with depression severity and increase in response to antidepressant treatment in animal models of depression [54, 55]. Intriguingly, periodontitis, either independently or comorbid with other conditions such as diabetes, may impact dendritic arborization [56, 57].

With the objective of obtaining a deeper understanding of the association between periodontitis and depression, a secondary analysis of our previously published studies [12, 13], is presented aiming to conduct an extensive morphological and inflammatory phenotypic analysis of the microglial population, elucidating potential

alterations in the expression and intracellular signaling of ECs and proteins associated with synaptic plasticity in the FC of rats exposed to a combined model of both comorbidities.

## Materials & methods

### Animals

This study adhered to the modified ARRIVE guidelines 2.0 for preclinical in vivo research [58] and conformed to the regulatory standards outlined by Spanish and European Union regulations (European Communities Council Directive 86/609/EEC). The in vivo experimental segment of the study was conducted at the Experimental Animal Center of the Complutense University of Madrid, following the approval of its protocol by the regional authorities (PROEX 087/18) and the Ethical Committee of Animal Experimentation.

Male Wistar Hannover rats (HsdRccHan: Wist, from Envigo, Spain) with body weights ranging from 230 to 280 g were housed in a controlled environment at a constant temperature of  $24 \pm 2$  °C and a relative humidity of  $70 \pm 5\%$ , following a 12-h light-dark cycle (lights on at 8:00 AM). Throughout the experimental procedures, the rats had free access to fresh tap water and were provided ad libitum access to standard pellet chow (A04 SAFE, Scientific Animal Food and Engineering, Augy, France). All animals were acclimatized under constant conditions and handled daily for 7 days before the experiments.

### Experimental protocol

The following four experimental groups exhibited different combinations of periodontitis (P) and chronic mild stress (CMS): (a) the control group (P-CMS-); (b) the periodontitis group (P+CMS-); (c) the CMS group (P-CMS+) and (d) the periodontitis and CMS group (P+CMS+). The induction of periodontitis preceded

exposure to chronic mild stress (CMS) (Fig. 1). Both in vivo protocols have been previously reported and validated individually [59, 60] and in combination [12, 13], including the periodontal outcomes and behavioral results of the experimental groups used in this study [13].

The experimental periodontitis model consisted of 12 weeks of oral gavage (4 times per week) of inoculation with two recognized periodontal pathogens, *P. gingivalis* ATCC W83K1 and *F. nucleatum* DMSZ 20,482. These bacteria were given to the animals in a viscous solution (2% carboxymethylcellulose) that allows bacteria to adhere to the various structures of the oral cavity. Although some of the solution may potentially reach the intestine, most of it remains on the teeth and it is expelled from the mouth again, thanks to the action of the syringe (the rat cannot keep the entire volume in its mouth and swallow it directly). Furthermore, bacteria rarely colonize healthy guts, even if swallowed, due to gastrointestinal tract barriers, the presence of the resident gut microbiota, and the acidity of the stomach, especially considering the absence of antibiotic treatment previous to periodontitis induction in our experimental setting [11].

The CMS paradigm encompasses a diverse array of stressors, including [a] food deprivation, [b] water deprivation, [c] cage tilting, [d] soiled cages, [e] grouped housing after a period of water deprivation, [f] stroboscopic illumination [150 flashes/min], and [g] intermittent illumination every 2 h. These stressors were changed daily (two stressors/day) and administered unpredictably for 21 days, with an additional day to maintain stress exposure during subsequent behavioral tests [13].

Forty-eight male rats were randomly allocated to each group ( $n=12$  rats/group), underwent a 7-day acclimatization period, and subjected to the experimental procedures. Two rats died after anesthesia administration at baseline (P-CMS- group), and two died following

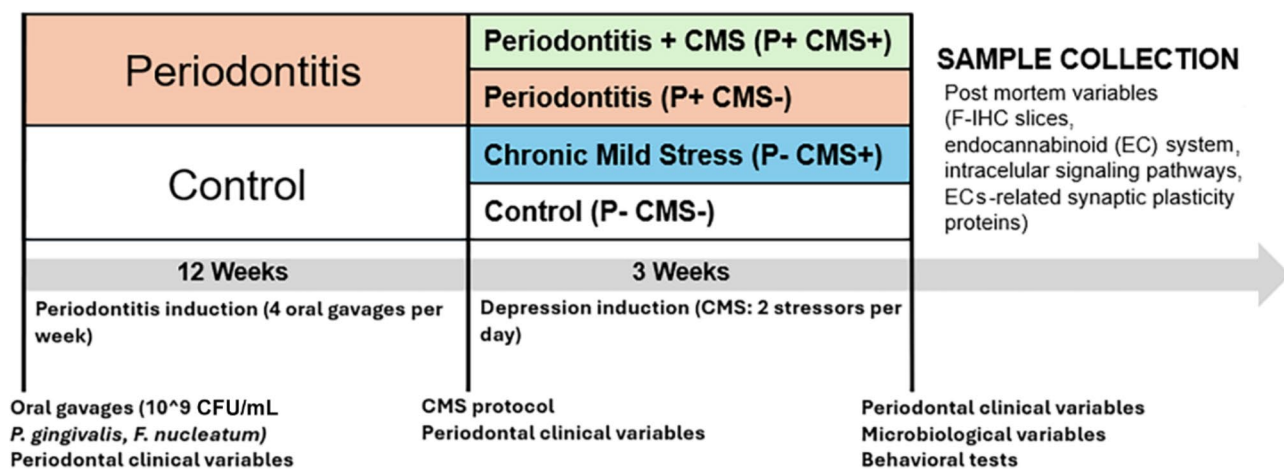


**Fig. 1** Experimental protocol. Induction of periodontitis in Wistar male rats via experimental oral gavage with a solution of periodontal bacteria (12 weeks) and subsequent exposure to a model of chronic mild stress (3 weeks) [13]. CFU: colony-forming unit, F-IHC: fluorescence immunohistochemistry

periodontitis induction (P+CMS- and P-CMS+ groups). Overall, forty-four rats completed the in vivo experimental phase. Among these, twelve were used for fluorescence immunohistochemistry (F-IHC) ( $n=3$  rats/group), while the remaining thirty-six were used for biochemical assays ( $n=7-9$  rats/group).

### Tissue specimens

Samples were collected following terminal anesthesia after the last stress session utilizing sodium pentobarbital (320 mg/kg i.p.; Vetoquinol®, Madrid, Spain). Anesthesia was consistently administered between 2:00 and 3:00 PM to mitigate potential alterations arising from circadian rhythm fluctuations. The animals were divided into two distinct sets for F-IHC and biochemical analyses.

For F-IHC, rats were perfused via the ascending aorta, initially with 200 ml of saline solution, followed by perfusion with 200 ml of 4% paraformaldehyde (PFA) in 0.1 M phosphate-buffered saline (PBS) (pH 7.4). Subsequently, the brains were collected, postfixed in 4% PFA overnight at 4 °C, cryoprotected with 30% sucrose, and frozen. Coronal sections of 30 µm from the FC were obtained using a microtome and stored at -40 °C immersed in a cryopreserving solution.

For biochemical analyses, the brain was harvested after decapitation, and the left hemisphere FC was dissected and immediately frozen at -80 °C. Total homogenates and nuclear extracts were prepared from FC tissue. For total homogenates, FC tissue was homogenized in 1× PBS (pH=7) supplemented with a protease inhibitor cocktail (Complete Roche, Basel, Switzerland) using Tissue-Lyser LT (QIAGEN, Hilden, Germany) at 50/s for 4 min, followed by centrifugation at 19,083 g for 10 min. The resulting supernatant served as the FC protein extract for western blot analysis. A modified procedure based on the method of Schreiber et al. [61] was employed to obtain nuclear extracts.

### Fluorescence immunohistochemistry (F-IHC)

Three slices of the anteroposterior stereotaxic coordinates from bregma 2.7, 1.7, and 1.2 mm were employed for F-IHC analyses. Antigen retrieval involved subjecting the sections to a sodium citrate solution at pH 6.0 for 40 min within a temperature range of 40 °C to 65 °C. The sections were subsequently washed with 0.02 M potassium phosphate-buffered saline (KPBS), immersed in 0.1 M glycine for 20 min to eliminate autofluorescence, washed with KPBS, and blocked for 60 min with 10% bovine serum albumin (BSA) in KPBS containing 0.1% Triton X-100. Next, the sections were incubated overnight with primary antibodies in 10%-BSA KPBS, washed again, incubated with secondary antibodies in 10%-BSA KPBS, and ultimately mounted with Fluoroshield containing 40,6-diamidino-2-phenylindole dihydrochloride

(DAPI). Antibody titration to prevent nonspecific interactions and negative controls for each antibody were used to confirm the absence of nonspecific fluorescent signals. Four to six 20× confocal images per section were acquired using an FV1200 confocal Olympus microscope (Olympus, Shinjuku, Tokyo, Japan) at the CAI-UCM Flow Cytometry and Fluorescence Microscopy Unit.

### Microglial morphological analysis

The primary antibody used was anti-ionized calcium-binding adapter molecule 1 (Iba1) (ab108539, Abcam, dilution 1:1000), and the secondary antibody used for microglial morphological analysis was Alexa Fluor 555-conjugated donkey anti-rabbit (A31572, Life Technologies, dilution 1:1000).

One hundred forty-four microglia/group were evaluated (4 cells/microphotography × 4 microphotography/section × 3 section/rat × 3 rat/group=144 cell/group). The analysis was based on the protocol described by Vargas-Caraveo et al. [62] and executed using the Fiji ImageJ® package (NIH, Bethesda, MD, USA). The threshold was adjusted to obtain binary images, and each cell was selected using the region of interest (ROI). The extra signal was removed to generate a single-cell image of microglia. The outlined and skeletonized formats of the new single-cell binary files were used for fractal and skeleton analyses, respectively.

Fractal analysis was performed on the outlined cells using the FracLac plugin, with Num G set to 4 and the metric box checked from the binary image. The outlined cells were scanned to obtain hull and circle results, selecting the span ratio, area, and circularity. The soma area was calculated using ROIs. Fractal dimension, lacunarity, and density were selected in the Box count summary, providing insights into microglial shape (elongated or round) and complexity. Cell skeletonized images were analyzed using the Analyze-Skeleton plugin, the skeleton option was selected, and the branch information box was checked. The results showed the number and length of branches.

### Inducible nitric oxide synthase (iNOS) and CB2 microglial expression

For the analysis of iNOS microglial expression, the primary antibodies used were anti-iNOS (BD610329 BD Biosciences, 1:1000) and anti-Iba1, and the secondary antibodies used were Alexa Fluor 488-conjugated goat anti-mouse (A11001, Life Technologies, 1:1000) and Alexa Fluor 555-conjugated goat anti-rabbit, respectively. For the analysis of CB2 microglial expression, the primary antibodies used were anti-CB2 (sc-10076 Santa Cruz, 1:500) and anti-Iba1, and the secondary antibodies used were Alexa Fluor 488-conjugated donkey anti-goat

(A11055, Life Technologies, 1:1000) and Alexa Fluor 555-conjugated goat anti-rabbit, respectively.

Thirty-six neurons/group were analyzed (4 microphotography/section  $\times$  3 section/rat  $\times$  3 rat/group=36 microphotography/group). A threshold was applied to gray images to identify the number of Iba1+ cells. iNOS or CB2 fluorescence intensity was the ratio between the general mean value of the iNOS or CB2 signal and the number of parenchymal microglia (Iba1+ cells) in the image.

#### **CB1 neuronal expression**

For the analysis of CB1 neuronal expression, the primary antibodies used were anti-CB1 (ab23703 Abcam, 1:1000) and anti-neuronal nuclear antigen (NeuN) (ab23703 Abcam, 1:1000), and the secondary antibodies used were Alexa Fluor 488-conjugated donkey anti-rabbit (A21206, Life Technologies, 1:1000) and Alexa Fluor 555-conjugated goat anti-mouse (A21422, Life Technologies, 1:1000), respectively.

Fifty-four neurons/group were analyzed (6 microphotography/section  $\times$  3 section/rat  $\times$  3 rat/group=54 microphotography/group). A threshold was applied to gray images to obtain the number of NeuN+ cells. CB1 fluorescence intensity was the ratio between the general mean value of the CB1 signal and the number of neurons (NeuN+ cells) in the image.

#### **Western blot**

Protein levels in FC homogenates were quantified using the Bradford method based on the principle of protein-dye binding. Subsequently, 15  $\mu$ g of protein was mixed with Laemmli sample buffer (Bio-Rad, Hercules, CA, USA) and loaded and size separated by 8% sodium dodecyl sulfate-polyacrylamide gel electrophoresis (90 V). The gel contents were then transferred to nitrocellulose membranes using the Trans-Blot Turbo Transfer System (Bio-Rad, Hercules, CA, USA).

The membranes were blocked in Tris-buffered saline (TBS) containing 0.1% Tween 20 and 5% BSA for 1 h and incubated overnight at 4 °C with specific primary antibodies against PLD-NAPE (10306 Cayman Chemical, 1:1000), DAGL (sc-133307 Santa-Cruz Biotechnology 1:750, 2% BSA), FAAH (101600 Cayman Chemical 1:1000), MAGL (100035 Cayman Chemical, 1:1000), CB1 (ab23703 Abcam, 1:1000), PI3K (sc7189 Santa Cruz 1:1000, 5% BSA), phospho(p)-Akt (4060 Cell Signaling, 1:1000, BSA 2.5%), Akt (4691 Cell Signaling, 1:2000, BSA 2.5%), p-ERK (8544 Cell Signaling, 1:1000), ERK (4695 Cell Signaling, 1:1000), p-CREB (9198 Cell Signaling, 1:1000), CREB (9197 Cell Signaling, 1:1000), BDNF (ab108319 Abcam, 1:1000, BSA 2.5%), TrkB (ab18987 Abcam, 1:1000, BSA 5%), and synaptophysin (S5768 Sigma Aldrich 1:2000).

Following primary antibody incubation, the membranes were washed and incubated with the appropriate horseradish peroxidase-conjugated secondary antibodies (anti-rabbit IgG, 7074; Cell Signaling, 1:2000; anti-mouse sc516102; Santa Cruz, 1:2000; BSA, 2.5%) for 90 min at room temperature. Finally, the membranes were developed using the ECL Prime kit following the manufacturer's instructions (Cytiva Marlborough, MA, USA). Blots were imaged using a ChemiDoc™ (Bio-Rad®, Hercules, CA, USA) and quantified by densitometry with the Fiji ImageJ® package.

All densitometry data were obtained in arbitrary optical density units and are expressed as a percentage of the control group (100%). Multiple exposure times ensured the linearity of the band intensities. Beta-actin (A5441 Sigma, 1:10000) was used as the loading control for cytosolic extract samples, and GAPDH (G8795 Sigma, 1:5000) was used for nuclear extracts.

#### **Statistical analysis**

Details regarding the sample size calculations are provided in Martínez et al. [13]. In summary, a total of 48 animals (12 animals per group) were evaluated for a difference of 1.6 $\times$  sigma in the protein expression of molecules associated with neuroinflammation, with a standard deviation (SD) of 25 [59]. A subset of 12 animals (3 animals per group) was subjected to immunofluorescence studies.

The animal was used as the unit of analysis. The data are presented as the mean  $\pm$  standard error of the mean (SEM). The Grubbs test identified significant outliers at  $\alpha=0.05$ , allowing for the exclusion of one value per group. The normality of the distribution was assessed using the Shapiro–Wilk test, and variables were also checked for homogeneity of variance by the Brown–Forsythe test. When the data exhibited a Gaussian distribution and equal variances, one-way ANOVA followed by a Tukey post hoc test for multiple comparisons was applied. In cases where SDs were unequal, a Brown–Forsythe ANOVA test followed by Tamhane's T2 post hoc test was used. For nonnormally distributed data, variables were log-transformed. If the data did not follow a Gaussian distribution after transformation, a nonparametric Kruskal–Wallis test with Dunn's multiple comparisons was used for the original data. A  $p$  value  $\leq 0.05$  was considered to indicate statistical significance. The data were analyzed using GraphPad Prism 9 (GraphPad Software, San Diego, CA, USA).

## **Results**

### **Microglial morphological analysis**

Skeletal and fractal analyses provided insights into the morphological properties of microglia through

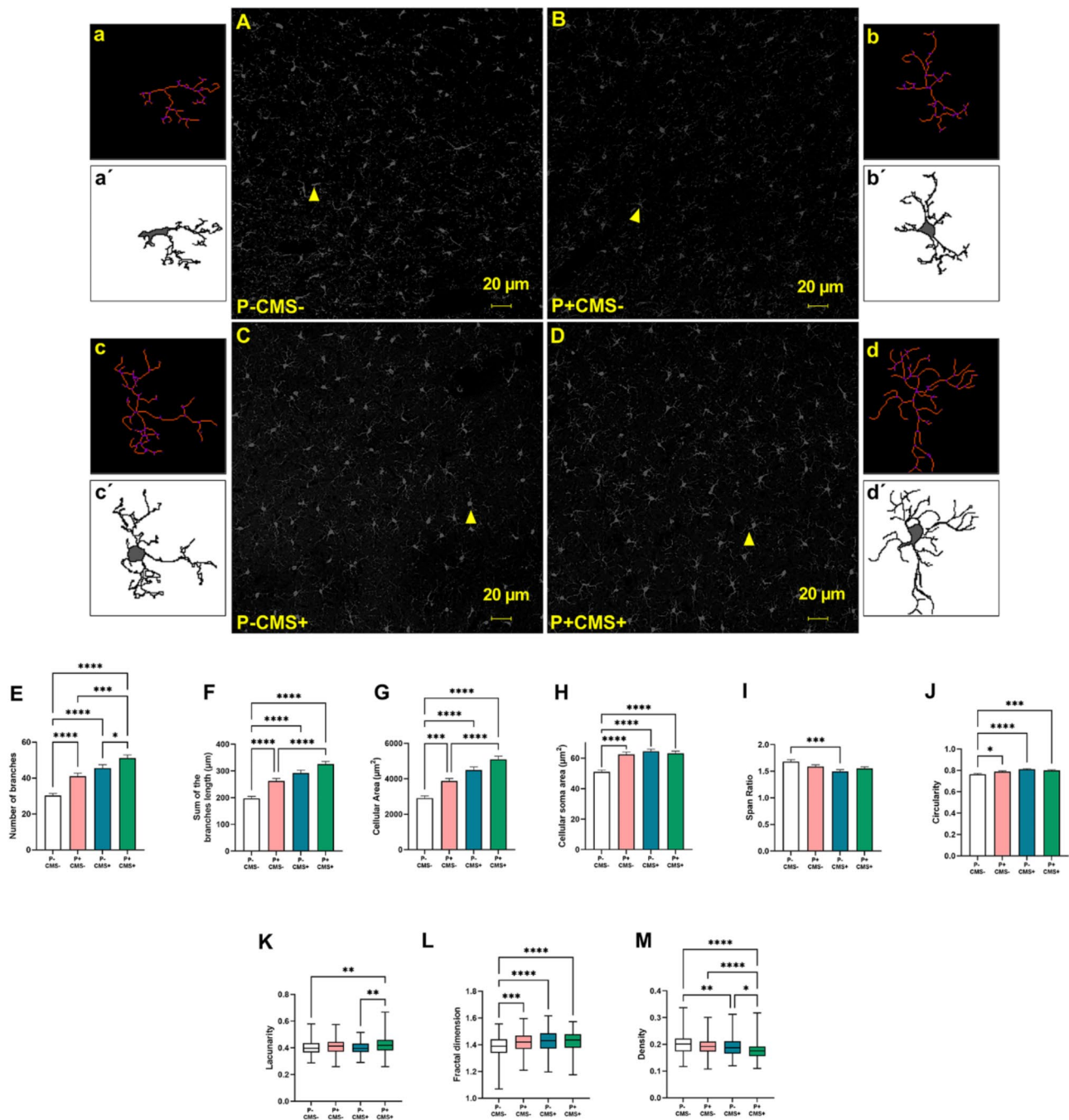


**Fig. 2** Analysis of microglial morphology in the FC of rats in control conditions (P-CMS-) after periodontitis induction (P+CMS-), after chronic mild stress exposure (P-CMS+), and after both protocols combined (P+CMS+). Immunofluorescence of Iba-1 in representative images of 30 μm-thick sections. (P-CMS-) (A), (P+CMS-) (B), (P-CMS+) (C), and (P+CMS+) (D) skeletonized and binaries outlined images of the microglia mentioned above. Yellow arrowheads indicate representative cells. Statistical analysis of the number of microglial branches (E), the sum of branch length (F), cell area (G), cellular soma area (H), span ratio (I), circularity (J), lacunarity (K), fractal dimension (L) and density (M). The data are presented as the means ± SEMs of 144 microglia per group. \* $p < 0.05$ ; \*\* $p < 0.01$ ; \*\*\* $p < 0.001$ ; \*\*\*\* $p < 0.0001$ . Scale bars = 20 μm. One-way ANOVA with Tukey's post hoc test for the cellular soma area and the Kruskal–Wallis test with Dunn's post hoc test were used for the remaining parameters

skeletonized (Fig. 2a-d) and outlined (Fig. 2a'-d') shapes (Fig. 2A-D).

Skeleton analysis revealed alterations in the number and length of microglial branches (Fig. 2E-F), revealing a

significant increase in the number of microglial branches across all experimental groups compared to the control group ( $p < 0.0001$ ) (Fig. 2E). Notably, the group with the greatest number of branches was P+CMS+. The sum of

the branch lengths exhibited a similar pattern ( $p < 0.0001$ ) (Fig. 2F).

A battery of parameters (cellular area, soma area, span ratio, circularity, lacunarity, fractal dimension, and density) (Fig. 2G–M) further characterized the morphology of parenchymal microglia in the FC. The cellular area increased in every group compared to that in the control group ( $p < 0.001$  vs. P+CMS-,  $p < 0.0001$  vs. P-CMS+,  $p < 0.0001$  vs. P+CMS+), with P+CMS+ displaying the greatest increase (Fig. 2G). Similarly, compared with that in the control group, the soma area in the covered surface in all the experimental groups significantly increased ( $p < 0.0001$ ), but no differences were detected among them (Fig. 2H).

The span ratio, a parameter that measures elongation, was significantly lower in the P-CMS+ group than in the control group ( $p < 0.001$ ) (Fig. 2I). The circumference of microglia increased in every experimental group compared to that in the control group ( $p < 0.05$  vs. P+CMS-,  $p < 0.0001$  vs. P-CMS+,  $p < 0.001$  vs. P+CMS+) (Fig. 2J).

Lacunarity indicates morphological heterogeneity and was greater in the P+CMS+ group than in the control ( $p < 0.01$ ) and P-CMS+ ( $p < 0.01$ ) groups (Fig. 2K). Fractal dimension and density, defined as the foreground/hull area ratio, assess complexity (Fig. 2L–M). The fractal dimension revealed greater complexity of microglia in all experimental groups than in the control group ( $p < 0.001$  vs. P+CMS-,  $p < 0.0001$  vs. P-CMS+,  $p < 0.0001$  vs. P+CMS+) (Fig. 2L). The density was lower in the P-CMS+ ( $p < 0.01$ ) and P+CMS+ ( $p < 0.0001$ ) groups than in the control group. Importantly, this parameter was even lower in the P+CMS+ group than in the P-CMS+ group ( $p < 0.05$ ), emphasizing the heightened complexity of microglia in the P+CMS+ group.

### Pro/antiinflammatory phenotype of parenchymal microglia

Following the comprehensive characterization of parenchymal microglial morphology, our focus shifted to their pro/antiinflammatory phenotype within our experimental groups. We investigated the expression of the proinflammatory enzyme iNOS in microglia [63] (Fig. 3A–D). iNOS immunoreactivity was significantly greater in the P+CMS+ group than in the control group ( $p < 0.001$ ) (Fig. 3E).

CB2 is a typical anti-inflammatory factor in microglia [64], and we studied its expression (Fig. 4A–D). CB2 immunoreactivity decreased in the P-CMS+ group compared to the control group (Fig. 4E,  $p < 0.01$ ).

### Metabolism of ECs

The unexpected outcomes observed for CB2 in P+CMS+ microglia prompted an exploration into the metabolic enzymes and signaling of ECs, as this system

may contribute (at least partially) to the regulatory effects exerted by microglia on various neurophysiological processes [65, 66], including neuroplasticity mediated through neuronal CB1 [67–69].

The enzyme responsible for AEA synthesis, NAPE-PLD, exhibited a greater reduction in the P+CMS+ group than in the control ( $p < 0.05$ ) and P+CMS- ( $p < 0.01$ ) groups (Fig. 5A). DAGL, at the helm of 2-AG synthesis, decreased in the P+CMS+ group compared to the P+CMS- group ( $p < 0.01$ ) (Fig. 5B). The activity of the AEA degradation enzyme FAAH decreased in the P+CMS+ group compared to the P+CMS- group (Fig. 5C). MAGL is the main enzyme for 2-AG metabolism and exhibited lower protein levels in the P+CMS+ group than in the P-CMS+ group ( $p < 0.01$ ) (Fig. 5D). Overall, the protein expression of synthesis and degradation enzymes in ECs decreased in the FC of P+CMS+ rats.

Given that the CB1 receptor predominantly mediates EC functions in the CNS, including the induction of neuroplasticity, we investigated its expression in FC sections from the different experimental groups by immunofluorescence. We found predominant expression in neurons (NeuN+ cells) (Fig. 6A–D). Further analysis revealed that CB1 neural expression was lower in the P+CMS+ group than in the other groups ( $p < 0.0001$ ) (Fig. 6E). Complementary analysis of CB1 protein expression by WB in FC samples also revealed lower levels in the P+CMS+ group than in the control group ( $p < 0.05$ ) (Fig. 6F).

### Intracellular signaling pathways related to CB1 modulation of neuroplasticity

PI3K/Akt and ERK1-2/CREB are cannabinoid intracellular signaling pathways that control synaptic plasticity. The protein levels of PI3K in the FC samples were significantly lower in the two groups exposed to chronic stress (P-CMS+ and P+CMS+) than in the P+CMS- group ( $p < 0.05$ ) (Fig. 7A). The p-Akt/Akt ratio was lower in the P+CMS+ group than in the control ( $p < 0.01$ ) and P+CMS- ( $p < 0.01$ ) groups (Fig. 7B).

Concerning ERK1-2/CREB, the pERK/ERK ratio was lower in the P+CMS+ group than in the control group ( $p < 0.05$ ) (Fig. 7C). However, the pCREB/CREB ratio remained unaltered across groups (Fig. 7D).

### Synaptic plasticity proteins

BDNF and synaptophysin are pivotal proteins in synaptic plasticity. BDNF protein levels decreased in the P+CMS+ group compared to those in the other groups ( $p < 0.05$  vs. P-CMS-,  $p < 0.01$  vs. P+CMS-,  $p < 0.0001$  vs. P-CMS+) (Fig. 8A). The level of the active form of the TrkB receptor, which transduces the BDNF signal, increased in the P+CMS- group compared to the control ( $p < 0.01$ ) and P+CMS+ ( $p < 0.01$ ) groups



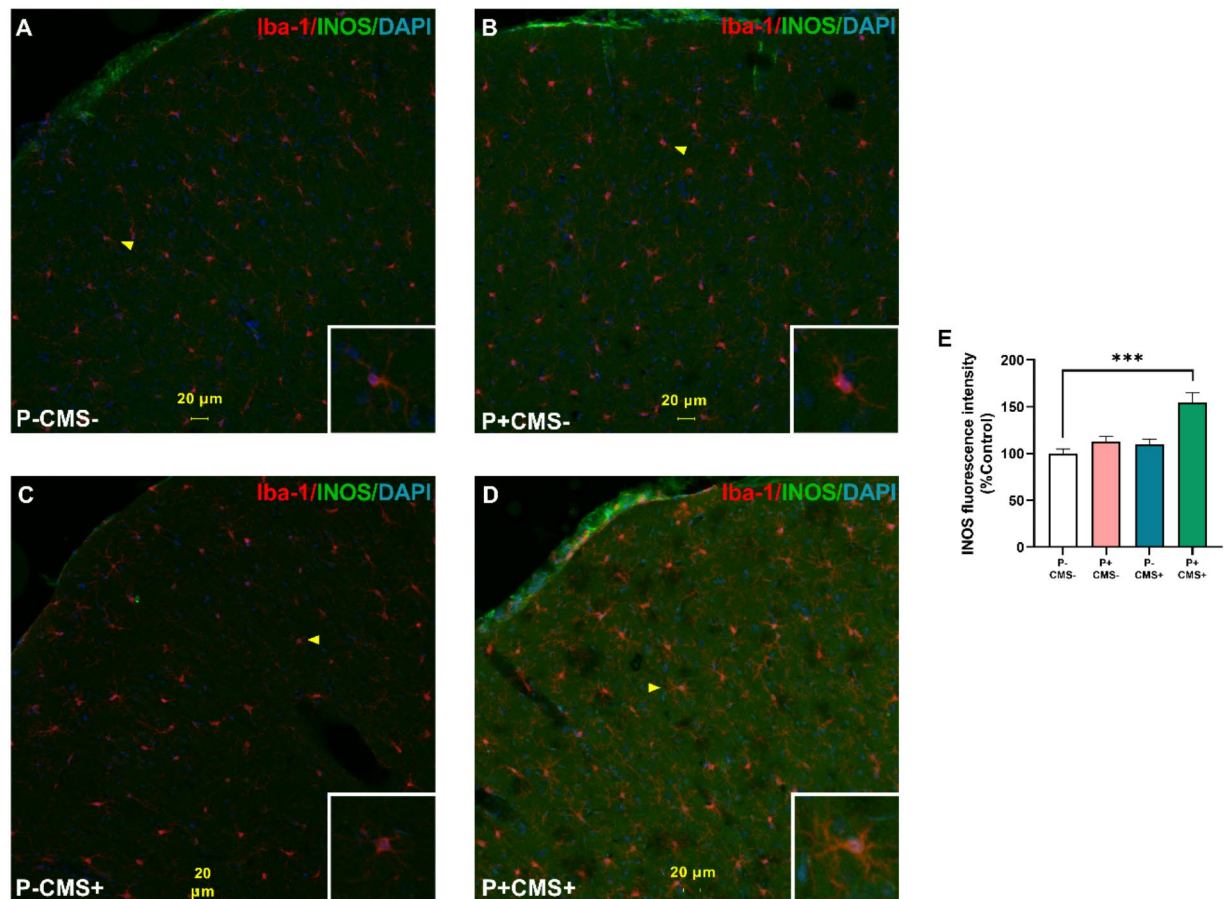


**Fig. 3** iNOS immunoreactivity in parenchymal microglia of the FC of rats in control conditions (P-CMS-), after periodontitis induction (P+CMS-), after chronic mild stress exposure (P-CMS+), and after both protocols combined (P+CMS+). Immunofluorescence of Iba1 (red), iNOS (green), and 4',6-diamidino-2-phenylindole dihydrochloride (DAPI) in nuclei (blue) was performed in representative images of 30 μm-thick sections of rat brain FC from the P-CMS- (A), P+CMS- (B), P-CMS+ (C), and P+CMS+ (D) groups. Arrowheads indicate representative cells. Quantitative analysis of iNOS expression in Iba1+ cells (E). The data are presented as the means ± SEMs of 34–36 microglia per group. \*\*\* $p < 0.001$ . Kruskal–Wallis test with Dunn's post hoc test. Scale bars = 20 μm

(Fig. 8B). Notably, the expression pattern of synaptophysin mirrored that of BDNE, with a decrease in the P+CMS+ group compared to the control ( $p < 0.01$ ) and P-CMS+ ( $p < 0.01$ ) groups (Fig. 8C).

## Discussion

The results from this investigation revealed a cascade of deleterious effects within the FC of rats exposed to a combined model of periodontitis and depression (Graphical Abstract). P+CMS+ animals displayed notable alterations in microglial morphology, inflammatory phenotype, EC metabolism and signaling, and proteins related to synaptic plasticity. These alterations were more noticeable when both diseases were present, which may explain the behavioral impairments previously reported in the P+CMS+ group [13].

The computational approach applied [62, 70] described structural alterations in microglia across all experimental

groups, characterized by a greater cell and soma size and a general increase in the number and length of branches. These changes were more pronounced in the combined P+CMS+ group.

Furthermore, lacunarity and fractal dimension notably increased in the P+CMS+ group. Lacunarity, which is associated with soma size, reflects the heterogeneity or rotational variability of a cell, with higher values indicating increased heterogeneity [71]. Similarly, higher fractal dimension values suggest greater structural complexity [71]. These parameters provide complementary information, allowing the discernment of differences between P-CMS+ and P+CMS+ that might otherwise go unnoticed [72]. Additionally, density decreased in the P+CMS+ group compared to all the other groups, indicating higher levels of structural complexity. All these results imply the existence of a hyperbranched phenotype among microglia in our experimental groups [73].

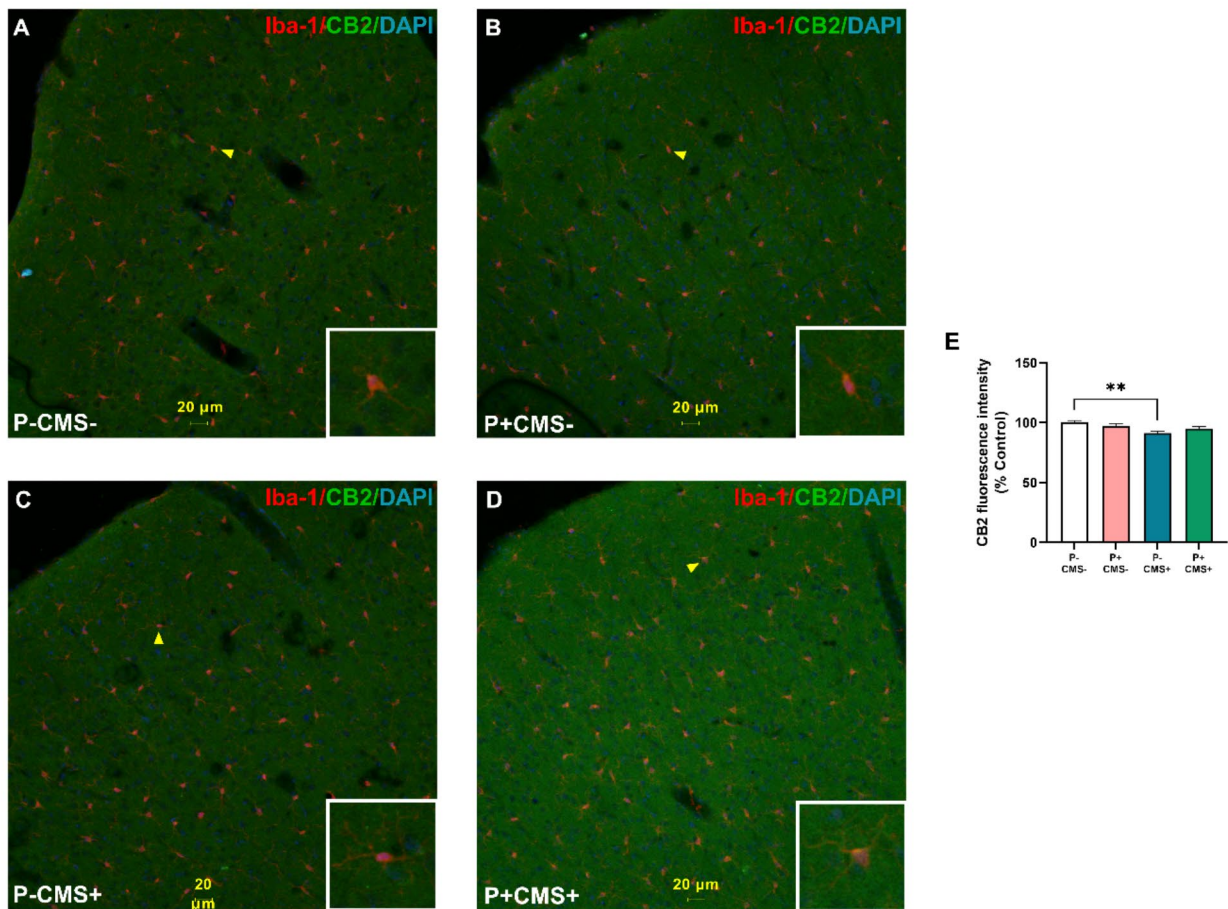


**Fig. 4** CB2 immunoreactivity in parenchymal microglia of the FC of rats in control conditions (P-CMS-), after periodontitis induction (P+CMS-), after chronic mild stress exposure (P-CMS+), and after both protocols combined (P+CMS+). Immunofluorescence of Iba1 (red), CB2 (green) and 4',6-diamidino-2-phenylindole dihydrochloride (DAPI) signals in nuclei (blue) in representative images of 30 μm-thick sections of rat brain FC from the P-CMS- (A), P+CMS- (B), P-CMS+ (C), and P+CMS+ (D) groups was performed. Arrowheads indicate representative cells. Quantitative analysis of CB2 expression in Iba1+ cells (E). The data are presented as the means ± SEMs of 34–36 microglia per group. \*\* $p < 0.01$ . One-way ANOVA was performed following Tukey's post hoc test. Scale bars = 20 μm

This phenotype, previously observed in murine models of chronic stress [74, 75], appears to be closely linked to depressive-like behaviors [76].

A branched microglial phenotype in rats was also evident in rats subjected solely to periodontitis (P+CMS-), aligning with previous evidence reporting mild microglial activation in the prefrontal cortex and hippocampus in models involving exposure to LPS from *P. gingivalis* [17, 77]. Systemic *P. gingivalis* LPS can induce microglial activation at blood–brain interfaces, such as CVOs [62]. This activation of microglia is directly associated with the emergence of depressive-like behavior [78]. Interestingly, the antidepressant imipramine inhibits LPS-*P. gingivalis*-induced inflammatory responses in microglia and alleviates neuronal damage associated with periodontitis [79].

The analysis of the inflammatory state of microglia within our experimental groups revealed diverse activity states of microglia. P+CMS+ microglia exhibited

elevated iNOS expression, which indicates an elevated proinflammatory state. Previous findings in this combined in vivo model of periodontitis and depression revealed depressive-like behavior and neuroinflammation in the FC, with increased expression of tumor necrosis factor-α (TNF-α), interleukin-1 beta (IL-1β), Toll-like receptor 4 (TLR4), nuclear factor kappa B (NF-κB), iNOS, microsomal prostaglandin E synthase (mPGES), and phospho-p38 mitogen-activated protein kinase (p-p38) [13].

Compared with the controls, all the experimental groups demonstrated decreased expression of the anti-inflammatory marker CB2, although only in the P-CMS+ group there was statistically significant difference. Although specific studies examining the impact of periodontitis on CB2 expression in FC microglia are lacking, lower CB2 expression in human gingival biopsies has been reported [34, 35]. Our CB2 results underscore

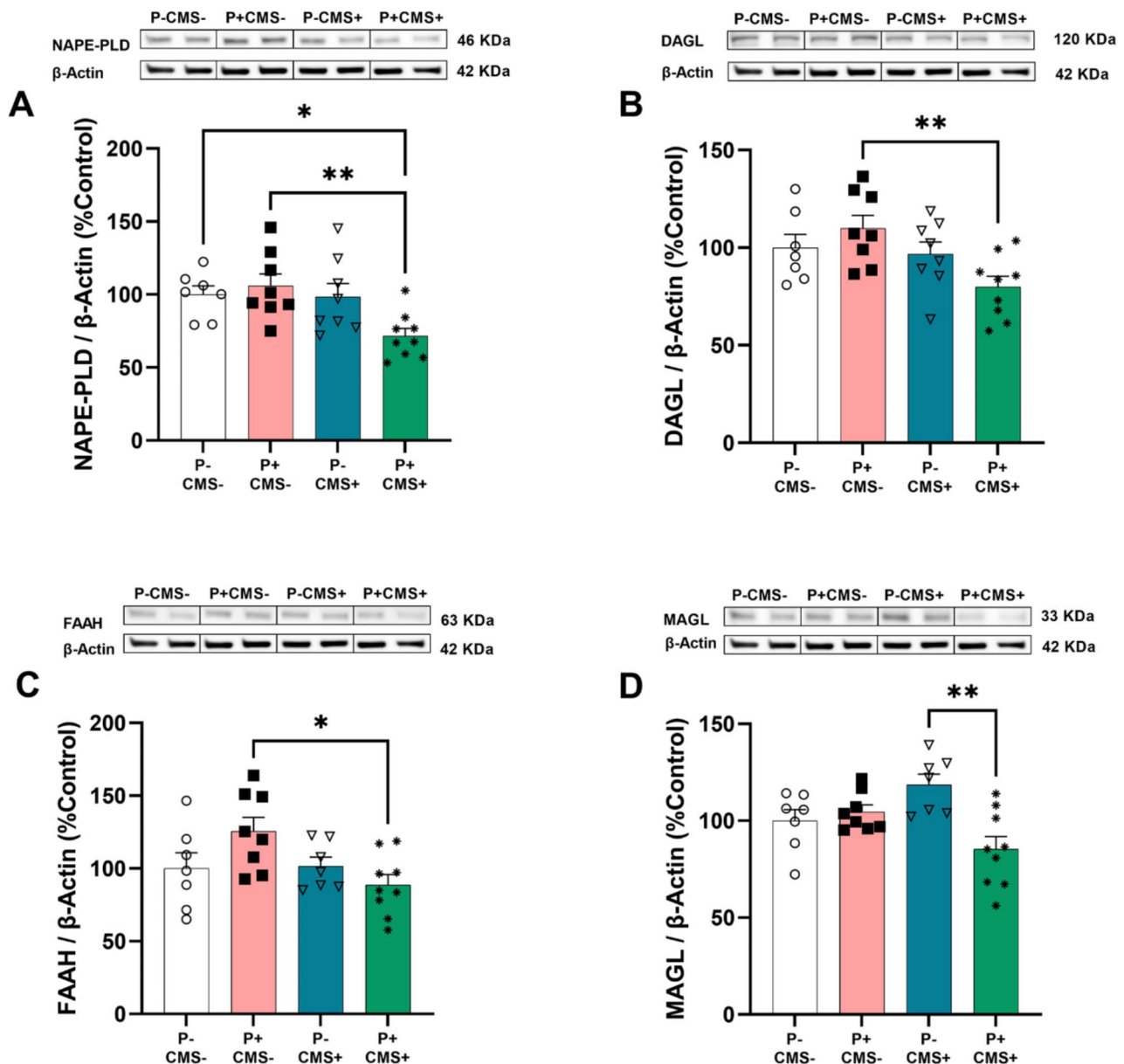


**Fig. 5** Endocannabinoid metabolism in the FC of rats in control conditions (P-CMS-), after periodontitis induction (P+CMS-), after chronic mild stress exposure (P-CMS+), and after both protocols combined (P+CMS+). Protein expression of N-acyl phosphatidylethanolamine-specific phospholipase D (NAPE-PLD) (A), diacylglycerol lipase (DAGL) (B), fatty acid amide hydrolase (FAAH) (C), and monoacylglycerol lipase (MAGL) (D) in FC samples by WB. The densitometric data of the band of interest were normalized to that of beta-actin ( $\beta$ -actin). The data are presented as the means  $\pm$  SEMs of 6–9 rats per group. \* $p < 0.05$ , \*\* $p < 0.01$ . One-way ANOVA with a Tukey post hoc test. Blots were cropped (black lines) to improve the clarity and conciseness of the presentation

the intricate nature of microglial states following consecutive immune challenges, emphasizing the necessity of employing multiple quantitative and qualitative approaches to comprehensively assess such complexity [80]. Indeed, microglial complexity and heterogeneity may not unequivocally align with a strictly pro- or anti-inflammatory phenotype and could drive other processes.

The initially unexpected result concerning neuroinflammation and CB2 microglial expression in

P+CMS+ animals prompted us to investigate the EC signaling in the FC due to the well-established ability of microglia to regulate other crucial cellular processes in the brain through ECs. Notably, such regulation has been documented following immune challenges with LPS and interferon-gamma (IFN- $\gamma$ ) [66], and both periodontitis and depression independently have demonstrated some effects on the EC system [28, 34, 41].

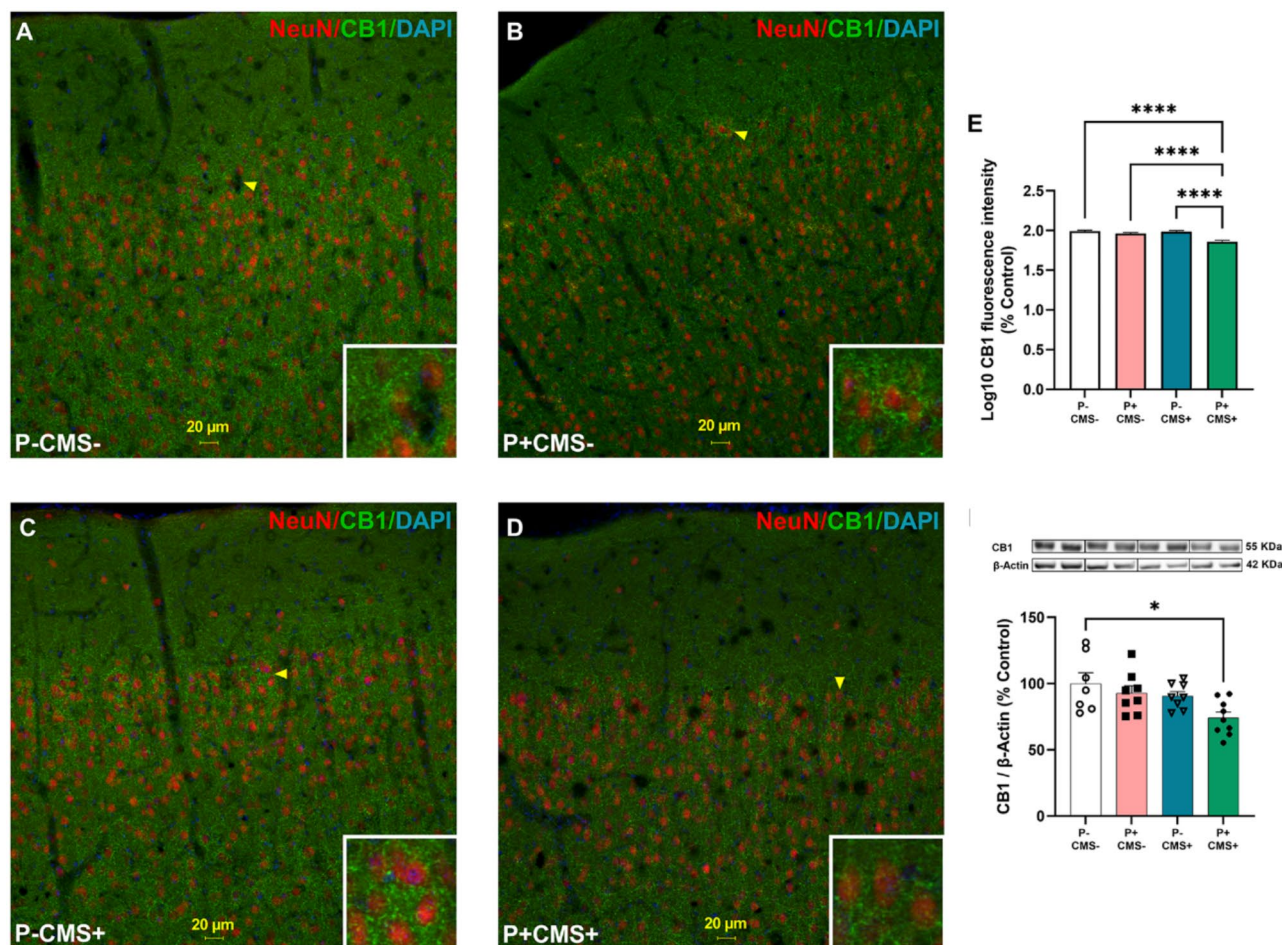


**Fig. 6** Cannabinoid receptor 1 (CB1) immunoreactivity in NeuN+ cells and CB1 expression by western blot (WB) in the frontal cortex (FC) of rats in control conditions (P-CMS-), after periodontitis induction (P+CMS-) after chronic mild stress exposure (P-CMS+), and after both protocols combined (P+CMS+). Immunofluorescence of NeuN (red), CB1 (green) and 4',6-diamidino-2-phenylindole dihydrochloride (DAPI) signals in nuclei (blue) in representative images of 30 mm-thick sections of rat brain FC from the P-CMS- (A), P+CMS- (B), P-CMS+ (C), and P+CMS+ (D) groups was performed. Arrowheads indicate representative cells. Quantitative analysis of CB1 expression in NeuN+ cells (E). The data are presented as the means  $\pm$  SEMs of 54 neurons per group. \*\*\*\* $p < 0.0001$ . Scale bars = 20  $\mu$ m. Protein expression of CB1 in FC samples by WB (F). The densitometric data of the band of interest were normalized to that of  $\beta$ -actin. The data are presented as the means  $\pm$  SEMs of 6–9 rats per group. \* $p < 0.05$ , \*\* $p < 0.01$ . One-way ANOVA with a Tukey post hoc test after logarithmic transformation. Blots were cropped (black lines) to improve the clarity and conciseness of the images

Neither periodontitis nor CMS altered the expression of EC enzymes in the FC in our experimental setting. However, the NAPE-PLD, DAGL, and MAGL were lower in the combined treatment group than in the control group. Particularly noteworthy was the significant downregulation of the synthesis enzyme NAPE-PLD without changes in the degradation enzyme FAAH, potentially leading to reduced AEA levels and the subsequent partial disruption of the homeostatic endocannabinergic tone in these animals. In line with this, previous research has reported antidepressant-like activity following FAAH inhibition in a rat model of CMS [81]. Moreover, an anti-inflammatory role for AEA has been documented in a combined model of experimental periodontitis induced by ligatures around the first inferior molars and immobilization stress for 2 h twice daily for 7 days [37]. Further

research must obtain direct evidence about the AEA and 2-AG levels to confirm the indirect evidence provided by the data from EC metabolic enzymes.

CB1 predominantly governs EC actions on neurons, particularly those related to plasticity. Immunofluorescence and expression analyses of total homogenates revealed a downregulation of CB1 in the P+CMS+ group. While there is no prior evidence regarding the impact of periodontitis on brain CB1, some research has indicated that periodontitis does not affect CB1 expression in human gingival biopsies [35]. In contrast, there is extensive information on the effect of chronic stress on CB1 in depression-like animal models. Chronic stress exposure can affect the EC signaling by reducing CB1 density in the hippocampus but not in the limbic forebrain [82]. Furthermore, CB1 knockout mice are more susceptible to

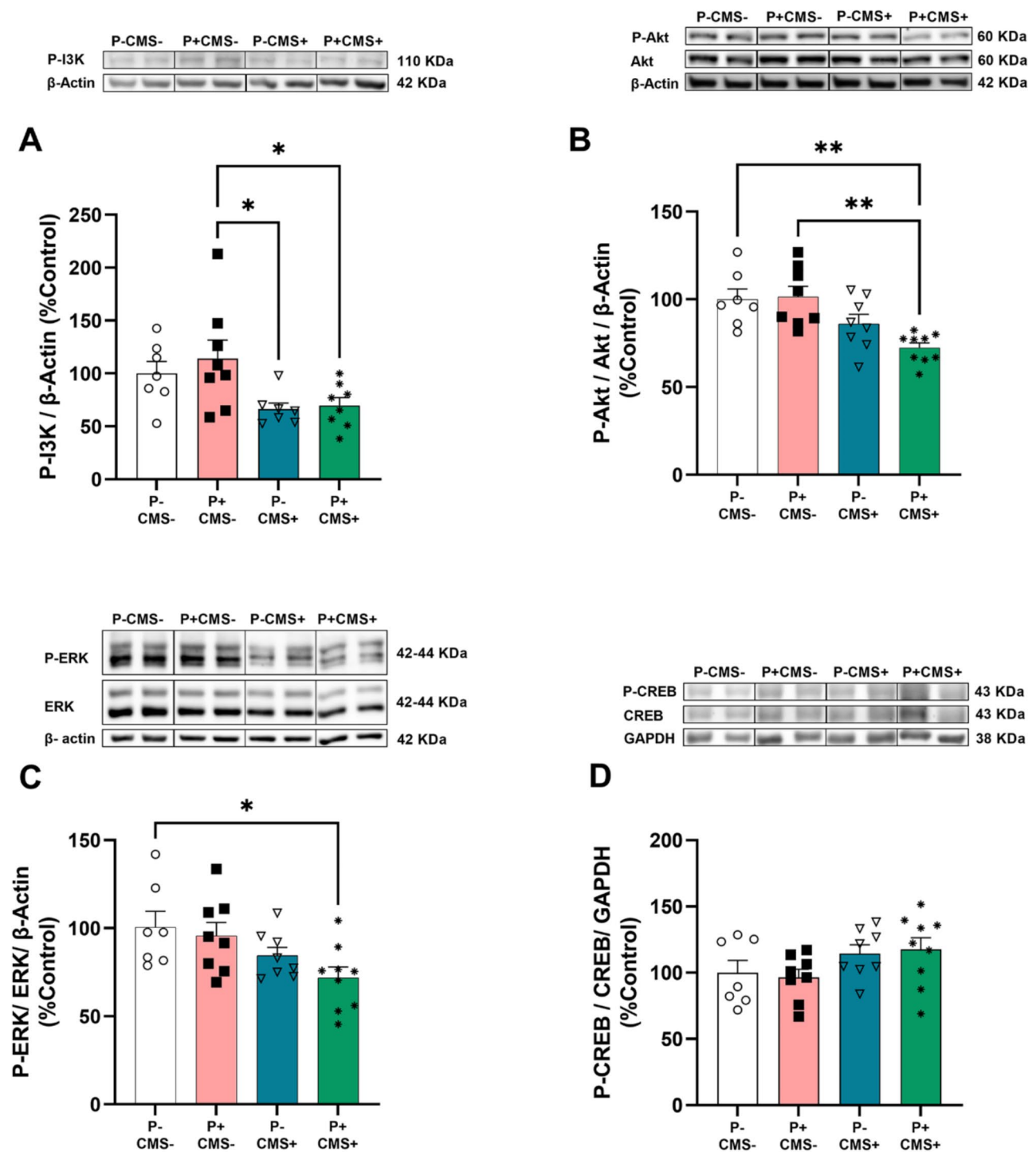


**Fig. 7** Intracellular signaling pathways in the frontal cortex (FC) of rats in control conditions (P-CMS-), after periodontitis induction (P+CMS-), after chronic mild stress exposure (P-CMS+), and after both protocols combined (P+CMS+). Protein expression of phosphatidylinositol-3-kinase (PI3K) (**A**), phospho-protein kinase B (p-Akt)/Akt ratio (**B**), p-extracellular signal-regulated kinase (p-ERK)/ERK ratio (**C**) and phospho-cAMP response element-binding protein (p-CREB)/CREB ratio (**D**) in FC samples by WB. The densitometric data of the band of interest were normalized to that of  $\beta$ -actin. The data are presented as the means  $\pm$  SEMs of 6–9 rats per group. \* $p < 0.05$ , \*\* $p < 0.01$ . One-way ANOVA with a Tukey post hoc test. Blots were cropped (black lines) to improve the clarity and conciseness of the images

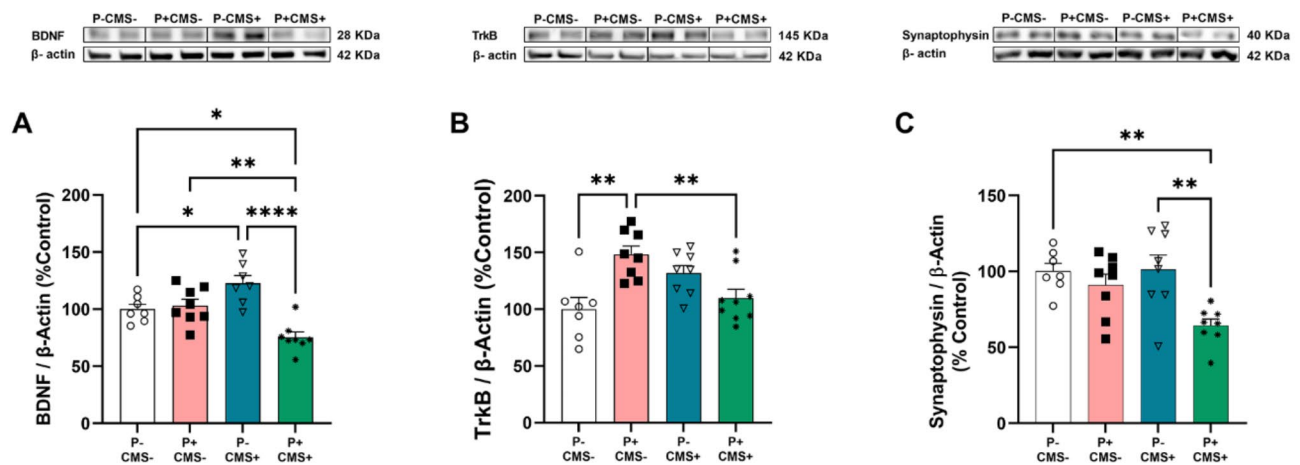


**Fig. 8** Synaptic plasticity markers in the frontal cortex (FC) of rats in control conditions (P-CMS-), after periodontitis induction (P+CMS-), after chronic mild stress exposure (P-CMS+), and after both protocols combined (P+CMS+). Protein expression of brain-derived neurotrophic factor (BDNF) (A), tropomyosin receptor kinase B (TrkB) (B) and synaptophysin (C) in FC samples by WB. The densitometric data of the band of interest were normalized to that of  $\beta$ -actin. The data are presented as the means  $\pm$  SEMs of 6–9 rats per group. \* $p < 0.05$ , \*\* $p < 0.01$ . One-way ANOVA with a Tukey post hoc test. Blots were cropped (black lines) to improve the clarity and conciseness of the images

developing depressive-like behavior after CMS exposure [83], and pharmacological modulation of CB1 prevents the effects of CMS on emotional learning and long-term potentiation [84].

The signal transduction of CB1 and other pathways related to inflammation requires the activity of PI3K/Akt and ERK1-2/CREB. Similar to the expression pattern of CB1, the levels of PI3K, Akt and ERK decreased exclusively in the P+CMS+ group compared to those in the control group. However, there were no discernible alterations in the p-CREB/CREB ratio across any of the experimental groups. Previously, our group reported a reduction in PI3K and Akt in FC samples following CMS exposure [85], consistent with the outcomes observed in P-CMS+ animals. Although no *in vivo* studies have detailed changes in these molecules in the brain during periodontitis, an *in vitro* study indicated that microglia stimulated with gingipains exhibited activation of protease-activated receptor 2, leading to subsequent activation of the PI3K/Akt and ERK pathways [86]. Our results are not specific to microglia and revealed no alterations in the expression of these pathways in P+CMS- animals.

CB1 signaling plays a pivotal role in regulating synaptic plasticity, and activation of the PI3K/Akt and ERK/CREB pathways has been implicated in this neuroprotective response by activating promoter 4 of the BDNF gene [87, 88]. Consequently, genetic deletion and pharmacological inhibition of these pathways downregulate BDNF synthesis, leading to reduced cell survival and the onset of working and long-term memory alterations [89]. The P+CMS+ group exhibited lower levels of BDNF, consistent with this plausible pathological scenario occurring in our combined model of periodontitis and depression. Indeed, *P. gingivalis* can induce depressive-like behavior

by downregulating p75NTR-mediated BDNF maturation in astrocytes [90].

Controversially, BDNF increased in the P-CMS+ animals in our experimental setting. Many papers have described a reduction in BDNF levels related to depression and associated its increase with antidepressant response [91, 92]. Still, other studies from depression models have reported no changes or increased BDNF expression in different brain areas [93–96], with more consistent results of the BDNF reduction in the hippocampus than in the frontal cortex ([97]. A possible explanation for the increased BDNF detected in the frontal cortex relies on a decreased turnover of BDNF leading to higher non-released tissue levels, differential stress effects between the hippocampus and the frontal cortex, or compensatory mechanisms due to cortex-hippocampal projections [98]. Interestingly, BDNF in different areas of the frontal cortex was only upregulated after antidepressant treatment and remained unchanged in MDD drug-free patients [99], suggesting a role of BDNF in antidepressant effects rather than as a pathophysiological feature of depression in this cerebral area.

Our results did not show changes in neuroplasticity molecules in the P-CMS+ group. Nevertheless, we cannot ignore the temporal dynamics associated with BDNF expression [100] and the fact that we measured them at the time of sacrifice, which does not preclude that the neuroplasticity pathway was reduced any earlier time, potentially contributing to the behavioral impairments of P-CMS+ animals. Importantly, the decrease in the neuroplasticity pathway detected in the P+CMS+ group may aggravate the pathology [78, 101] or affect the potential pharmacological intervention with antidepressants when periodontitis is comorbid. Undoubtedly, further research

is warranted to continue delving into the mechanisms of BDNF in depression and its contribution to the disease.

TrkB transduces the BDNF signal by activating cAMP kinases, ultimately regulating the expression of synaptophysin [89, 102]. Despite unaltered TrkB levels across all experimental groups, the level of synaptophysin decreased in the P+CMS+group. Synaptophysin plays a role in establishing and maintaining synaptic connections and regulating neurotransmitters within the synaptic space. Reduced synaptophysin expression is associated with synaptic impairment in the hippocampus [103]. Moreover, the administration of cannabidiol in murine models increased the mRNA expression levels of synaptophysin in the medial prefrontal cortex, resulting in antidepressant effects [104]. Animals solely exposed to periodontitis in our experimental setting did not exhibit changes in synaptophysin levels. However, other researchers have reported that systemic *P. gingivalis* infection increases the expression of IL-1 $\beta$  in leptomeninges while simultaneously decreasing the expression of synaptophysin in the cortex adjacent to leptomeninges in mice [105].

This investigation tackles the difficulties in addressing the combination of periodontitis and depression from a preclinical perspective by attempting to decipher the contribution of a brain cell type, microglia. Nonetheless, certain limitations warrant acknowledgment. First, the descriptive nature of our study is not sufficient to draw a consistent chronological pathway from microglial to plasticity alterations for a mechanistic explanation. Second, the analysis of the metabolic enzymes of the EC system provides only indirect evidence regarding the levels of AEA and 2-AG. Third, the findings in plasticity suggest that behavioral tests focused on cognition would have helped assess the repercussions of the observed molecular changes.

## Conclusions

In conclusion, the results from this investigation revealed more pronounced alterations in the microglial phenotype, the EC signaling, and proteins associated with synaptic plasticity in animals exposed to periodontitis and CMS. This evidence underscores the potential of pharmacological interventions targeting these pathways in patients suffering from both conditions. In fact, a recent systematic review with meta-analysis explored the potential beneficial use of antidepressant agents in managing periodontitis [106], and other reports investigated the potential of infection control measures to treat periodontitis to ameliorate depressive-like symptoms [11]. These insights suggest promising avenues associated with microglia, the EC signaling, and plasticity for addressing the intricate interplay in the comorbidity between oral health and psychiatric disorders.

## Abbreviations

2-AG	2-arachidonoylglycerol
AEA	Anandamide
Akt	Protein kinase B
BBB	Blood–brain barrier
BDNF	Brain-derived neurotrophic factor
BSA	Bovine serum albumin
CB	Cannabinoid receptor
CMS	Chronic mild stress
CNS	Central nervous system
CREB	cAMP response element-binding protein
DAGL	Diacylglycerol lipase
EC	Endocannabinoid
ERK	Extracellular signal-regulated kinase
F. nucleatum	Fusobacterium nucleatum
FAAH	Fatty acid amide hydrolase
FC	Frontal cortex
F-IHC	Fluorescence immunohistochemistry
GAPDH	Glyceraldehyde-3-phosphate dehydrogenase
Iba1	Anti-ionized calcium-binding adapter molecule 1
iNOS	Inducible nitric oxide synthase
KPBS	Potassium phosphate-buffered saline
MAGL	Monoacylglycerol lipase
MAPKs	Mitogen-activated protein kinases
MDD	Major depressive disorder
NAPE	N-acyl phosphatidylethanolamine phospholipase
<i>P. gingivalis</i>	<i>Porphyromonas gingivalis</i>
PBS	Phosphate-buffered saline
PFA	Paraformaldehyde
PI3K	Phosphatidylinositol-3-kinase
ROI	Region of interest
SEM	Standard error of the mean
TrkB	Tropomyosin receptor kinase B

## Supplementary Information

The online version contains supplementary material available at <https://doi.org/10.1186/s12974-024-03213-5>.

Supplementary Material 1

## Acknowledgements

The authors thank the Experimental Animal Center (Centro de Asistencia a la Investigación (CAI) Animalario), Complutense University, Madrid, for the care and maintenance of the animals that were used in this study. Karina S. MacDowell is acknowledged for her support in administrative tasks.

## Author contributions

All the authors conceived and planned the experiments. NA and MJM prepared the oral gavage solutions. DMH, MM, LV, and EM performed the preclinical interventions in the animals. JRM, CDG, MML, BGB, and DMH carried out the immunohistochemical and biochemical analyses. JRM performed the computational analysis of the microglial phenotype. JRM, CDG, BGB, and DMH performed the statistical analyses. DH, MS, JCL, BGB, EF, and DMH contributed to the interpretation of the results. JRM, BGB, and DMH wrote the manuscript. All authors discussed and reviewed the manuscript.

## Funding

This study was funded through a research grant from Santander-University Complutense of Madrid Projects in 2017 (PR41/17–20979; principal investigator: Elena Figuero), by MINECO-FEDER Funds (PID2019-109033RB-I00 and PID2022-137932NB-I00 principal investigators: Juan Carlos Leza and Elena Figuero), and CIBERSAM/ISCIII.

## Data availability

The datasets used and/or analyzed during the current study are available from the corresponding author upon reasonable request.

## Declarations

### Ethical approval

This study was designed according to the modified ARRIVE guidelines 2.0 for preclinical in vivo research [58] and following Spanish and European Union regulations (European Communities Council Directive 86/609/EEC). The in vivo experimental part of the study was carried out in the Experimental Animal Center of the Complutense University of Madrid after its protocol was approved by the regional authorities (PROEX 087/18) and the Ethical Committee of Animal Experimentation.

### Consent for publication

Not applicable.

### Competing interests

The authors declare no competing interests.

### Author details

<sup>1</sup>Department of Pharmacology and Toxicology, School of Medicine, Faculty of Medicine, Complutense University of Madrid (UCM), Hospital 12 de Octubre Research Institute (Imas12), Neurochemistry Research Institute UCM (IUIIN), Pza. Ramón y Cajal s/n, Madrid 28040, Spain

<sup>2</sup>Biomedical Network Research Center of Mental Health (CIBERSAM), Institute of Health Carlos III, Madrid, Spain

<sup>3</sup>ETEP (Etiology and Therapy of Periodontal and Peri-Implant Diseases) Research Group, Complutense University of Madrid, Madrid, Spain

<sup>4</sup>Department of Dental Clinical Specialties, School of Dentistry, Faculty of Dentistry, Complutense University of Madrid, Pza. Ramón y Cajal s/n, Madrid 28040, Spain

<sup>5</sup>Department of Anatomy and Embryology, Faculty of Optics, Complutense University of Madrid, Madrid, Spain

Received: 7 March 2024 / Accepted: 29 August 2024

Published online: 08 September 2024

## References

- Otte C, Gold SM, Penninx BW, Pariante CM, Etkin A, Fava M, Mohr DC, Schatzberg AF. Major depressive disorder. *Nat Reviews Disease Primers*. 2016;2:16065.
- GBD: Global Burden of Disease Study 2019. (GBD 2019) Results tool. Seattle, United States of America: Institute for Health Metrics and Evaluation (IHME); 2021.
- World Health A. Global burden of mental disorders and the need for a comprehensive, coordinated response from health and social sectors at the country level: report by the Secretariat. Geneva: World Health Organization; 2012.
- Yuan K, Zheng YB, Wang YJ, Sun YK, Gong YM, Huang YT, Chen X, Liu XX, Zhong Y, Su SZ, et al. A systematic review and meta-analysis on prevalence of and risk factors associated with depression, anxiety and insomnia in infectious diseases, including COVID-19: a call to action. *Mol Psychiatry*. 2022;27:3214–22.
- Greenberg P, Chitnis A, Louie D, Suthoff E, Chen SY, Maitland J, Gagnon-Sanschagrin P, Fournier AA, Kessler RC. The Economic Burden of Adults with Major Depressive Disorder in the United States (2019). *Adv Ther*. 2023.
- Jaffe DH, Rive B, Deneer TR. The humanistic and economic burden of treatment-resistant depression in Europe: a cross-sectional study. *BMC Psychiatry*. 2019;19:247.
- Pérez-Sola V, Roca M, Alonso J, Gabilondo A, Hernando T, Sicras-Mainar A, Sicras-Navarro A, Herrera B, Vieta E. Economic impact of treatment-resistant depression: a retrospective observational study. *J Affect Disord*. 2021;295:578–86.
- Fries GR, Saldana VA, Finnstein J, Rein T. Molecular pathways of major depressive disorder converge on the synapse. *Mol Psychiatry*. 2023;28:284–97.
- Sorrells SF, Caso JR, Munhoz CD, Sapolsky RM. The stressed CNS: when glucocorticoids aggravate inflammation. *Neuron*. 2009;64:33–9.
- Chen X, Yao T, Cai J, Fu X, Li H, Wu J. Systemic inflammatory regulators and 7 major psychiatric disorders: a two-sample mendelian randomization study. *Prog Neuropsychopharmacol Biol Psychiatry*. 2022;116:110534.
- Martínez M, Postolache TT, García-Bueno B, Leza JC, Figuero E, Lowry CA, Malan-Müller S. The role of the oral microbiota related to Periodontal diseases in anxiety, Mood and Trauma- and stress-related disorders. *Front Psychiatry*. 2022;12:814177.
- Martín-Hernández D, Martínez M, Robledo-Montaña J, Muñoz-López M, Virto L, Ambrosio N, Marín MJ, Montero E, Herrera D, Sanz M et al. Neuroinflammation related to the blood-brain barrier and sphingosine-1-phosphate in a pre-clinical model of periodontal diseases and depression in rats. *J Clin Periodontol*. 2023.
- Martínez M, Martín-Hernández D, Virto L, MacDowell KS, Montero E, González-Bris Á, Marín MJ, Ambrosio N, Herrera D, Leza JC, et al. Periodontal diseases and depression: a pre-clinical in vivo study. *J Clin Periodontol*. 2021;48:503–27.
- Serrats J, Schiltz JC, García-Bueno B, van Rooijen N, Reyes TM, Sawchenko PE. Dual roles for perivascular macrophages in immune-to-brain signaling. *Neuron*. 2010;65:94–106.
- Li H, Sagar AP, Kéri S. Microglial markers in the frontal cortex are related to cognitive dysfunctions in major depressive disorder. *J Affect Disord*. 2018;241:305–10.
- Brás JP, Guillot de Suduiraut I, Zanoletti O, Monari S, Meijer M, Grosse J, Barbosa MA, Santos SG, Sandi C, Almeida MI. Stress-induced depressive-like behavior in male rats is associated with microglial activation and inflammation dysregulation in the hippocampus in adulthood. *Brain Behav Immun*. 2022;99:397–408.
- Almarhoumi R, Alvarez C, Harris T, Tognoni CM, Paster BJ, Carreras I, Dedeoglu A, Kantarci A. Microglial cell response to experimental periodontal disease. *J Neuroinflammation*. 2023;20:142.
- Wang H, He Y, Sun Z, Ren S, Liu M, Wang G, Yang J. Microglia in depression: an overview of microglia in the pathogenesis and treatment of depression. *J Neuroinflammation*. 2022;19:132.
- Yirmiya R. Depressive disorder-Associated Microglia as a target for a Personalized Antidepressant Approach. *Biol Psychiatry*. 2023;94:602–4.
- Enache D, Pariante CM, Mondelli V. Markers of central inflammation in major depressive disorder: a systematic review and meta-analysis of studies examining cerebrospinal fluid, positron emission tomography and post-mortem brain tissue. *Brain Behav Immun*. 2019;81:24–40.
- He L, Zheng Y, Huang L, Ye J, Ye Y, Luo H, Chen X, Yao W, Chen J, Zhang JC. Nrf2 regulates the arginase 1(+) microglia phenotype through the initiation of TREM2 transcription, ameliorating depression-like behavior in mice. *Transl Psychiatry*. 2022;12:459.
- Scheepstra KWF, Mizee MR, van Scheppingen J, Adelia A, Wever DD, Mason MRJ, Dubbelaar ML, Hsiao CC, Eggen BJL, Hamann J, Huitinga I. Microglia Transcriptional profiling in Major Depressive Disorder Shows Inhibition of Cortical Gray Matter Microglia. *Biol Psychiatry*. 2023;94:619–29.
- Setiawan E, Wilson AA, Mizrahi R, Rusjan PM, Miller L, Rajkowska G, Suridjan I, Kennedy JL, Rekkas PV, Houle S, Meyer JH. Role of Translocator Protein Density, a marker of Neuroinflammation, in the Brain during Major depressive episodes. *JAMA Psychiatry*. 2015;72:268–75.
- Paolicelli RC, Sierra A, Stevens B, Tremblay ME, Aguzzi A, Ajami B, Amit I, Audinat E, Bechmann I, Bennett M, et al. Microglia states and nomenclature: a field at its crossroads. *Neuron*. 2022;110:3458–83.
- Snijders G, Sneebouwer MAM, Fernández-Andreu A, Udine E, Boks MP, Ormel PR, van Berlekom AB, van Mierlo HC, Böttcher C, Priller J, et al. Distinct non-inflammatory signature of microglia in post-mortem brain tissue of patients with major depressive disorder. *Mol Psychiatry*. 2021;26:3336–49.
- Wohleb ES, Terwilliger R, Duman CH, Duman RS. Stress-Induced neuronal colony stimulating factor 1 provokes microglia-mediated neuronal remodeling and depressive-like Behavior. *Biol Psychiatry*. 2018;83:38–49.
- Marcaggi P, Attwells D. Endocannabinoid signaling depends on the spatial pattern of synapse activation. *Nat Neurosci*. 2005;8:776–81.
- Rodríguez-Muñoz M, Sánchez-Blázquez P, Callado LF, Meana JJ, Garzón-Niño J. Schizophrenia and depression, two poles of endocannabinoid system deregulation. *Transl Psychiatry*. 2017;7:1291.
- Garani R, Watts JJ, Mizrahi R. Endocannabinoid system in psychotic and mood disorders, a review of human studies. *Prog Neuropsychopharmacol Biol Psychiatry*. 2021;106:110096.
- Hill MN, Carrier EJ, McLaughlin RJ, Morrish AC, Meier SE, Hillard CJ, Gorzalka BB. Regional alterations in the endocannabinoid system in an animal model of depression: effects of concurrent antidepressant treatment. *J Neurochem*. 2008;106:2322–36.
- McPartland JM, Guy GW, Di Marzo V. Care and feeding of the endocannabinoid system: a systematic review of potential clinical interventions that upregulate the endocannabinoid system. *PLoS ONE*. 2014;9:e89566.



32. Arjmand S, Landau AM, Varastehmoradi B, Andreatini R, Joca S, Wegener G. The intersection of astrocytes and the endocannabinoid system in the lateral habenula: on the fast-track to novel rapid-acting antidepressants. *Mol Psychiatry*. 2022;27:3138–49.
33. Sharafi A, Pakkhesal S, Fakhari A, Khajehnasiri N, Ahmadelipour A. Rapid treatments for depression: endocannabinoid system as a therapeutic target. *Neurosci Biobehav Rev*. 2022;137:104635.
34. Pellegrini G, Carmagnola D, Toma M, Rasperini G, Orioli M, Dellavia C. Involvement of the endocannabinoid system in current and recurrent periodontitis: a human study. *J Periodontol Res*. 2023;58:422–32.
35. Ataei A, Rahim Rezaee SA, Moeintaghavi A, Ghanbari H, Azizi M. Evaluation of cannabinoid receptors type 1–2 in periodontitis patients. *Clin Exp Dent Res*. 2022;8:1040–4.
36. Nakajima Y, Furuichi Y, Biswas KK, Hashiguchi T, Kawahara K, Yamaji K, Uchimura T, Izumi Y, Maruyama I. Endocannabinoid, anandamide in gingival tissue regulates the periodontal inflammation through NF-kappaB pathway inhibition. *FEBS Lett*. 2006;580:613–9.
37. Rettori E, De Laurentis A, Zorrilla Zubilete M, Rettori V, Elverdin JC. Anti-inflammatory effect of the endocannabinoid anandamide in experimental periodontitis and stress in the rat. *Neuroimmunomodulation*. 2012;19:293–303.
38. Liu C, Qi X, Alhabeil J, Lu H, Zhou Z. Activation of cannabinoid receptors promote periodontal cell adhesion and migration. *J Clin Periodontol*. 2019;46:1264–72.
39. Yan W, Li L, Ge L, Zhang F, Fan Z, Hu L. The cannabinoid receptor 1 (CB1) enhanced the osteogenic differentiation of BMSCs by rescue impaired mitochondrial metabolism function under inflammatory condition. *Stem Cell Res Ther*. 2022;13:22.
40. Zhang F, Özdemir B, Nguyen PQ, Andrukhov O, Rausch-Fan X. Methanandamide diminish the Porphyromonas gingivalis lipopolysaccharide induced response in human periodontal ligament cells. *BMC Oral Health*. 2020;20:107.
41. Jäger A, Setiawan M, Beins E, Schmidt-Wolf I, Konermann A. Analogous modulation of inflammatory responses by the endocannabinoid system in periodontal ligament cells and microglia. *Head Face Med*. 2020;16:26.
42. Devane WA, Hanuš L, Breuer A, Pertwee RG, Stevenson LA, Griffin G, Gibson D, Mandelbaum A, Etinger A, Mechoulam R. Isolation and structure of a brain constituent that binds to the cannabinoid receptor. *Science*. 1992;258:1946–9.
43. Mechoulam R, Ben-Shabat S, Hanus L, Ligumsky M, Kaminski NE, Schatz AR, Gopher A, Almog S, Martin BR, Compton DR, et al. Identification of an endogenous 2-monoacylglyceride, present in canine gut, that binds to cannabinoid receptors. *Biochem Pharmacol*. 1995;50:83–90.
44. Matsuda LA, Lolait SJ, Brownstein MJ, Young AC, Bonner TI. Structure of a cannabinoid receptor and functional expression of the cloned cDNA. *Nature*. 1990;346:561–4.
45. Munro S, Thomas KL, Abu-Shaar M. Molecular characterization of a peripheral receptor for cannabinoids. *Nature*. 1993;365:61–5.
46. Maccarrone M, Di Marzo V, Gertsch J, Grether U, Howlett AC, Hua T, Makriyanis A, Piomelli D, Ueda N, van der Stelt M. Goods and bads of the Endocannabinoid System as a therapeutic target: lessons learned after 30 years. *Pharmacol Rev*. 2023;75:885–958.
47. Mackie K. Cannabinoid receptors: where they are and what they do. *J Neuroendocrinol*. 2008;20(Suppl 1):10–4.
48. Duffy SS, Hayes JP, Fiore NT, Moalem-Taylor G. The cannabinoid system and microglia in health and disease. *Neuropharmacology*. 2021;190:108555.
49. Malek N, Popiolek-Barczyk K, Mika J, Przewlocka B, Starowicz K. Anandamide, Acting via CB2 Receptors, Alleviates LPS-Induced Neuroinflammation in Rat Primary Microglial Cultures. *Neural Plast* 2015, 2015:130639.
50. Johannessen M, Delghandi MP, Moens U. What turns CREB on? *Cell Signal*. 2004;16:1211–27.
51. Innes S, Pariante CM, Borsini A. Microglial-driven changes in synaptic plasticity: a possible role in major depressive disorder. *Psychoneuroendocrinology*. 2019;102:236–47.
52. Wang T, Weng H, Zhou H, Yang Z, Tian Z, Xi B, Li Y. Esketamine alleviates postoperative depression-like behavior through anti-inflammatory actions in mouse prefrontal cortex. *J Affect Disord*. 2022;307:97–107.
53. Cheng CM, Hong CJ, Lin HC, Chu PJ, Chen MH, Tu PC, Bai YM, Chang WH, Juan CH, Lin WC, et al. Predictive roles of brain-derived neurotrophic factor Val66Met polymorphism on antidepressant efficacy of different forms of prefrontal brain stimulation monotherapy: a randomized, double-blind, sham-controlled study. *J Affect Disord*. 2022;297:353–9.
54. Kuwano N, Kato TA, Mitsuhashi M, Sato-Kasai M, Shimokawa N, Hayakawa K, Ohgidani M, Sagata N, Kubo H, Sakurai T, Kanba S. Neuron-related blood inflammatory markers as an objective evaluation tool for major depressive disorder: an exploratory pilot case-control study. *J Affect Disord*. 2018;240:88–98.
55. Varea E, Castillo-Gómez E, Gómez-Climent MA, Blasco-Ibáñez JM, Crespo C, Martínez-Guijarro FJ, Nàcher J. Chronic antidepressant treatment induces contrasting patterns of synaptophysin and PSA-NCAM expression in different regions of the adult rat telencephalon. *Eur Neuropsychopharmacol*. 2007;17:546–57.
56. Flores-Tochihuitl J, Márquez Villegas B, Peral Lemus AC, Andraca Hernández CJ, Flores G, Morales-Medina JC. Periodontitis and Diabetes reshape neuronal dendritic arborization in the thalamus and nucleus oralis in the rat. *Synapse*. 2021;75:e22187.
57. Xie C, Zhang Q, Ye X, Wu W, Cheng X, Ye X, Ruan J, Pan X. Periodontitis-induced neuroinflammation impacts dendritic spine immaturity and cognitive impairment. *Oral Dis* 2023.
58. Percie du Sert N, Ahluwalia A, Alam S, Avey MT, Baker M, Browne WJ, Clark A, Cuthill IC, Dirnagl U, Emerson M, et al. Reporting animal research: explanation and elaboration for the ARRIVE guidelines 2.0. *PLoS Biol*. 2020;18:e3000411.
59. Martín-Hernández D, Caso J, Bris Á, Maus S, Madrigal J, García-Bueno B, MacDowell K, Alou L, Gómez-Lus M, Leza J. Bacterial translocation affects intracellular neuroinflammatory pathways in a depression-like model in rats. *Neuropharmacology*. 2016;103:122–33.
60. Virto L, Cano P, Jiménez-Ortega V, Fernández-Mateos P, González J, Esquifino AI, Sanz M. Obesity and periodontitis: an experimental study to evaluate periodontal and systemic effects of comorbidity. *J Periodontol*. 2018;89:176–85.
61. Schreiber E, Matthias P, Müller MM, Schaffner W. Rapid detection of octamer binding proteins with 'mini-extracts', prepared from a small number of cells. *Nucleic Acids Res*. 1989;17:6419.
62. Vargas-Caraveo A, Sayd A, Robledo-Montaña J, Caso JR, Madrigal JLM, García-Bueno B, Leza JC. Toll-like receptor 4 agonist and antagonist lipopolysaccharides modify innate immune response in rat brain circumventricular organs. *J Neuroinflammation*. 2020;17:6.
63. Lisi L, Ciotti GM, Braun D, Kalinin S, Currò D, Dello Russo C, Coli A, Mangiola A, Anile C, Feinstein DL, Navarra P. Expression of iNOS, CD163 and ARG-1 taken as M1 and M2 markers of microglial polarization in human glioblastoma and the surrounding normal parenchyma. *Neurosci Lett*. 2017;645:106–12.
64. Komorowska-Müller JA, Schmöle AC. CB2 receptor in Microglia: the Guardian of Self-Control. *Int J Mol Sci* 2020, 22.
65. Morcuende A, García-Gutiérrez MS, Tambaro S, Nieto E, Manzanares J, Femenia T. Immunomodulatory Role of CB2 receptors in Emotional and Cognitive disorders. *Front Psychiatry*. 2022;13:866052.
66. Young AP, Denovan-Wright EM. The microglial endocannabinoid system is similarly regulated by lipopolysaccharide and interferon gamma. *J Neuroimmunol*. 2022;372:577971.
67. Tan H, Lauzon NM, Bishop SF, Bechard MA, Laviolette SR. Integrated cannabinoid CB1 receptor transmission within the amygdala-prefrontal cortical pathway modulates neuronal plasticity and emotional memory encoding. *Cereb Cortex*. 2010;20:1486–96.
68. Paes-Colli Y, Trindade PMP, Vitorino LC, Piscitelli F, Iannotti FA, Campos RMP, Isaac AR, de Aguiar AFL, Allodi S, de Mello FG, et al. Activation of cannabinoid type 1 receptor (CB1) modulates oligodendroglial process branching complexity in rat hippocampal cultures stimulated by olfactory ensheathing glia-conditioned medium. *Front Cell Neurosci*. 2023;17:1134130.
69. Molina-Holgado E, Vela JM, Arévalo-Martín A, Almazán G, Molina-Holgado F, Borrell J, Guaza C. Cannabinoids promote oligodendrocyte progenitor survival: involvement of cannabinoid receptors and phosphatidylinositol-3 kinase/Akt signaling. *J Neurosci*. 2002;22:9742–53.
70. Karperien AL, Jelinek HF. Fractal, multifractal, and lacunarity analysis of microglia in tissue engineering. *Front Bioeng Biotechnol*. 2015;3:51.
71. Fernández-Arjona MDM, Grondona JM, Fernández-Llebrez P, López-Avalos MD. Microglial morphometric parameters correlate with the expression level of IL-1 $\beta$ , and allow identifying different activated morphotypes. *Front Cell Neurosci*. 2019;13:472.
72. Karperien A, Ahammer H, Jelinek HF. Quantitating the subtleties of microglial morphology with fractal analysis. *Front Cell Neurosci*. 2013;7:3.
73. Vidal-Hiriago A, Radford RAW, Aramideh JA, Maurel C, Scherer NM, Don EK, Lee A, Chung RS, Graeber MB, Morsch M. Microglia morphophysiological diversity and its implications for the CNS. *Front Immunol*. 2022;13:997786.
74. Hinwood M, Tynan RJ, Charnley JL, Beynon SB, Day TA, Walker FR. Chronic stress induced remodeling of the prefrontal cortex: structural re-organization

- of microglia and the inhibitory effect of minocycline. *Cereb Cortex*. 2013;23:1784–97.
75. Walker FR, Nilsson M, Jones K. Acute and chronic stress-induced disturbances of microglial plasticity, phenotype and function. *Curr Drug Targets*. 2013;14:1262–76.
  76. Hellwig S, Brioschi S, Dieni S, Frings L, Masuch A, Blank T, Biber K. Altered microglia morphology and higher resilience to stress-induced depression-like behavior in CX3CR1-deficient mice. *Brain Behav Immun*. 2016;55:126–37.
  77. Mamunur R, Hashioka S, Azis IA, Jaya MA, Jerin SJF, Kimura-Kataoka K, Fujihara J, Inoue K, Inagaki M, Takeshita H. Systemic Administration of Porphyromonas Gingivalis Lipopolysaccharide induces glial activation and depressive-like Behavior in rats. *J Integr Neurosci*. 2023;22:120.
  78. Li Y, Guan X, He Y, Jia X, Pan L, Wang Y, Han Y, Zhao R, Yang J, Hou T. ProBDNF signaling is involved in periodontitis-induced depression-like behavior in mouse hippocampus. *Int Immunopharmacol*. 2023;116:109767.
  79. Yamawaki Y, So H, Oue K, Asano S, Furusho H, Miyauchi M, Tanimoto K, Kanematsu T. Imipramine prevents Porphyromonas gingivalis lipopolysaccharide-induced microglial neurotoxicity. *Biochem Biophys Res Commun*. 2022;634:92–9.
  80. Zhang Y, Cui D. Evolving models and tools for Microglial studies in the Central Nervous System. *Neurosci Bull*. 2021;37:1218–33.
  81. Bortolato M, Mangieri RA, Fu J, Kim JH, Arguello O, Duranti A, Tontini A, Mor M, Tarzia G, Piomelli D. Antidepressant-like activity of the fatty acid amide hydrolase inhibitor URB597 in a rat model of chronic mild stress. *Biol Psychiatry*. 2007;62:1103–10.
  82. Hill MN, Patel S, Carrier EJ, Rademacher DJ, Ormerod BK, Hillard CJ, Gorzalka BB. Downregulation of endocannabinoid signaling in the hippocampus following chronic unpredictable stress. *Neuropsychopharmacology*. 2005;30:508–15.
  83. Martin M, Ledent C, Parmentier M, Maldonado R, Valverde O. Involvement of CB1 cannabinoid receptors in emotional behaviour. *Psychopharmacology*. 2002;159:379–87.
  84. Segev A, Rubin AS, Abush H, Richter-Levin G, Akirav I. Cannabinoid receptor activation prevents the effects of chronic mild stress on emotional learning and LTP in a rat model of depression. *Neuropsychopharmacology*. 2014;39:919–33.
  85. Martin-Hernandez D, Bris AG, MacDowell KS, Garcia-Bueno B, Madrigal JL, Leza JC, Caso JR. Modulation of the antioxidant nuclear factor (erythroid 2-derived)-like 2 pathway by antidepressants in rats. *Neuropharmacology*. 2016;103:79–91.
  86. Liu Y, Wu Z, Nakanishi Y, Ni J, Hayashi Y, Takayama F, Zhou Y, Kadowaki T, Nakanishi H. Infection of microglia with Porphyromonas gingivalis promotes cell migration and an inflammatory response through the gingipain-mediated activation of protease-activated receptor-2 in mice. *Sci Rep*. 2017;7:11759.
  87. García-Gutiérrez MS, Ortega-Álvarez A, Busquets-García A, Pérez-Ortiz JM, Caltana L, Ricatti MJ, Brusco A, Maldonado R, Manzanares J. Synaptic plasticity alterations associated with memory impairment induced by deletion of CB2 cannabinoid receptors. *Neuropharmacology*. 2013;73:388–96.
  88. Blázquez C, Chiarlone A, Bellocchio L, Resel E, Pruunsild P, García-Rincón D, Sendtner M, Timmsk T, Lutz B, Galve-Roperh I, Guzmán M. The CB<sub>1</sub> cannabinoid receptor signals striatal neuroprotection via a PI3K/Akt/mTORC1/BDNF pathway. *Cell Death Differ*. 2015;22:1618–29.
  89. Bright U, Akirav I. Modulation of Endocannabinoid System Components in Depression: pre-clinical and clinical evidence. *Int J Mol Sci* 2022, 23.
  90. Wang YX, Kang XN, Cao Y, Zheng DX, Lu YM, Pang CF, Wang Z, Cheng B, Peng Y. Porphyromonas gingivalis induces depression via downregulating p75NTR-mediated BDNF maturation in astrocytes. *Brain Behav Immun*. 2019;81:523–34.
  91. Cavaleri D, Moretti F, Bartocchetti A, Mauro S, Crocama C, Carrà G, Bartoli F. The role of BDNF in major depressive disorder, related clinical features, and antidepressant treatment: insight from meta-analyses. *Neurosci Biobehav Rev*. 2023;149:105159.
  92. Hu X, Zhao HL, Kurban N, Qin Y, Chen X, Cui SY, Zhang YH. Reduction of BDNF Levels and Biphasic Changes in Glutamate Release in the Prefrontal Cortex Correlate with Susceptibility to Chronic Stress-Induced Anhedonia. *eNeuro* 2023, 10.
  93. Allaman I, Papp M, Kraftsik R, Fiumelli H, Magistretti PJ, Martin JL. Expression of brain-derived neurotrophic factor is not modulated by chronic mild stress in the rat hippocampus and amygdala. *Pharmacol Rep*. 2008;60:1001–7.
  94. Larsen MH, Mikkelsen JD, Hay-Schmidt A, Sandi C. Regulation of brain-derived neurotrophic factor (BDNF) in the chronic unpredictable stress rat model and the effects of chronic antidepressant treatment. *J Psychiatr Res*. 2010;44:808–16.
  95. Lin L, Herselman MF, Zhou XF, Bobrovskaya L. Effects of corticosterone on BDNF expression and mood behaviours in mice. *Physiol Behav*. 2022;247:113721.
  96. Schulte-Herbrüggen O, Fuchs E, Abumaria N, Ziegler A, Danker-Hopfe H, Hiemke C, Hellweg R. Effects of Escitalopram on the regulation of brain-derived neurotrophic factor and nerve growth factor protein levels in a rat model of chronic stress. *J Neurosci Res*. 2009;87:2551–60.
  97. Elfving B, Plougmann PH, Müller HK, Mathé AA, Rosenberg R, Wegener G. Inverse correlation of brain and blood BDNF levels in a genetic rat model of depression. *Int J Neuropsychopharmacol*. 2010;13:563–72.
  98. Dionisie V, Ciobanu AM, Toma VA, Manea MC, Baldea I, Olteanu D, Sevastre-Berghian A, Clichici S, Manea M, Riga S, Filip GA. Escitalopram targets oxidative stress, Caspase-3, BDNF and MeCP2 in the Hippocampus and Frontal Cortex of a rat model of Depression Induced by Chronic unpredictable mild stress. *Int J Mol Sci* 2021, 22.
  99. Sheldrick A, Camara S, Ilieva M, Riederer P, Michel TM. Brain-derived neurotrophic factor (BDNF) and neurotrophin 3 (NT3) levels in post-mortem brain tissue from patients with depression compared to healthy individuals - a proof of concept study. *Eur Psychiatry*. 2017;46:65–71.
  100. Caffino L, Mottarlini F, Piva A, Rizzi B, Fumagalli F, Chiamulera C. Temporal dynamics of BDNF signaling recruitment in the rat prefrontal cortex and hippocampus following a single infusion of a translational dose of ketamine. *Neuropharmacology*. 2024;242:109767.
  101. Ma X, Yoo JW, Shin YJ, Park HS, Son YH, Kim DH. Alleviation of Porphyromonas gingivalis or Its Extracellular Vesicles Provoked Periodontitis and Cognitive Impairment by Lactobacillus pentosus NK357 and Bifidobacterium bifidum NK391. *Nutrients* 2023, 15.
  102. Tartaglia N, Du J, Tyler WJ, Neale E, Pozzo-Miller L, Lu B. Protein synthesis-dependent and -independent regulation of hippocampal synapses by brain-derived neurotrophic factor. *J Biol Chem*. 2001;276:37585–93.
  103. Zhong Q, Xu H, Qin J, Zeng LL, Hu D, Shen H. Functional parcellation of the hippocampus from resting-state dynamic functional connectivity. *Brain Res*. 2019;1715:165–75.
  104. Xu C, Chang T, Du Y, Yu C, Tan X, Li X. Pharmacokinetics of oral and intravenous cannabidiol and its antidepressant-like effects in chronic mild stress mouse model. *Environ Toxicol Pharmacol*. 2019;70:103202.
  105. Huang W, Zeng F, Gu Y, Jiang M, Zhang X, Yan X, Kadowaki T, Mizutani S, Kashiwazaki H, Ni J, Wu Z. Porphyromonas Gingivalis infection induces synaptic failure via increased IL-1 $\beta$  production in Leptomeningeal cells. *J Alzheimers Dis*. 2021;83:665–81.
  106. Muniz F, Melo IM, Rösing CK, de Andrade GM, Martins RS, Moreira M, Carvalho RS. Use of antidepressive agents as a possibility in the management of periodontal diseases: a systematic review of experimental studies. *J Investig Clin Dent* 2018, 9.

## Publisher's note

Springer Nature remains neutral with regard to jurisdictional claims in published maps and institutional affiliations.